Search for Higgs pair production at the LHC Collider (CERN): The first measurement of the Higgs potential and search for new physics

Ph.D. thesis defence - 15 September 2021

Mohamed BELFKIR

Supervised by

Stéphane JEZEQUEL

ATLAS EXPERIMENT

LAPP
Laboratoire d'Annecy de Physique des Particules

UNIVERSITÉ SAVOIE MONT BLANC

Content

Content

The Standard Model (SM) of particle physics

- Quantum field theory, based on the principal gauge invariance $SU(3) \times SU(2) \times U(1)$
- Unify **Strong** and **Electro-weak** interactions
- **Fermions**: matter particles
  - **Quarks**
  - **Leptons**
- **Gauge bosons**: mediators of interactions
- **Higgs boson**: responsible for mass generation through EWSB mechanism

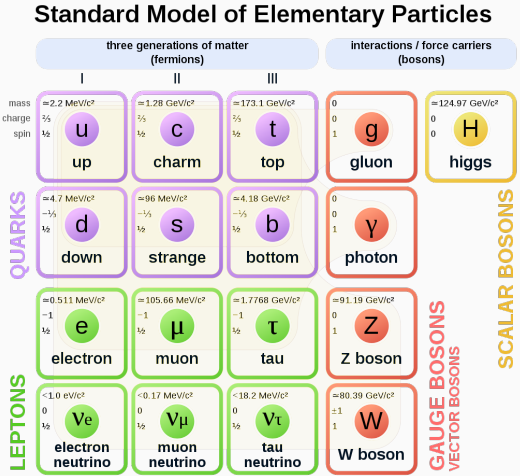

Electroweak Symmetry Breaking and Higgs boson

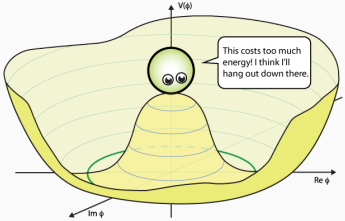

Gauge boson mass terms break gauge symmetry of SM

- Brout-Englert-Higgs (1964) include complex scalar field

$$V(\phi^\dagger\phi) = \mu^2\phi^\dagger\phi + \lambda(\phi^\dagger\phi)^2$$

$$\mu^2 < 0 \rightarrow \text{Mexican hat}$$

- Choice of the vacuum state v **spontaneously breaks the symmetry**
  - Gauge bosons become massive
  - **Higgs boson**: $m_H = -2\mu^2$
  - Fermion masses: generated through Yukawa couplings
- Observed in 2012 at LHC, $m_H \sim 125$ GeV

Electroweak Symmetry Breaking and Higgs boson

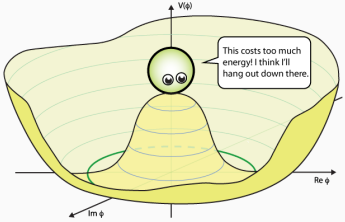

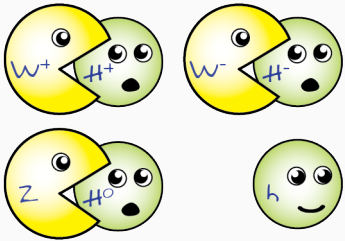

Gauge boson mass terms break gauge symmetry of SM

- Brout-Englert-Higgs (1964) include complex scalar field

$$V(\phi^\dagger\phi) = \mu^2\phi^\dagger\phi + \lambda(\phi^\dagger\phi)^2$$

$$\mu^2 < 0 \rightarrow \text{Mexican hat}$$

- Choice of the vacuum state v **spontaneously breaks the symmetry**
  - Gauge bosons become massive
  - **Higgs boson**: $m_H = -2\mu^2$
  - Fermion masses: generated through Yukawa couplings
- Observed in 2012 at LHC, $m_H \sim 125$ GeV

Measurements of Higgs parameters

mass

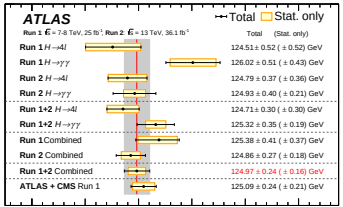

125.09 ± 0.24 GeV

cross-section

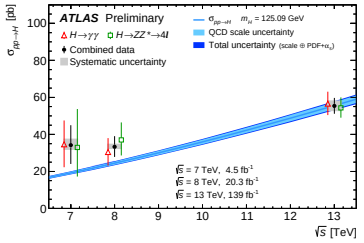

coupling

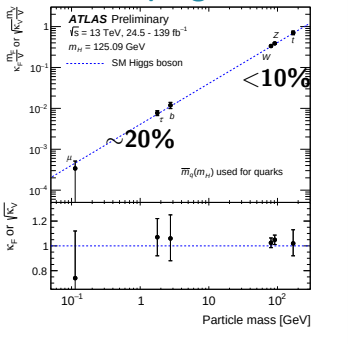

- Not all, Higgs boson self-coupling still resists to physicists

Measurements of Higgs parameters

mass

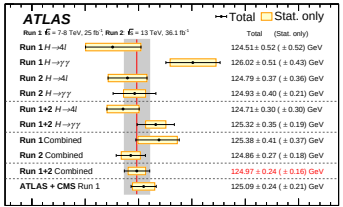

125.09 ± 0.24 GeV

cross-section

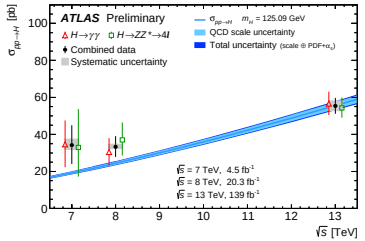

coupling

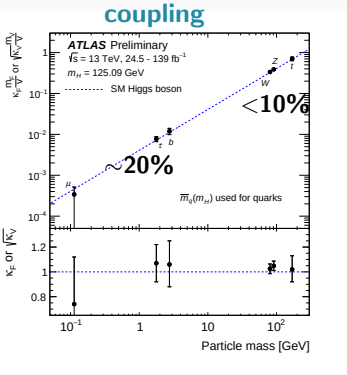

- Not all, Higgs boson self-coupling still resists to physicists

Higgs boson self-coupling

- **Self-coupling:** **Higgs boson trilinear coupling**
- Controls the shape of the Higgs potential
  - It is important to measure both m_H and λ
- **B**eyond **SM** (BSM) physics would impact this coupling, impact quantified as

$$\kappa_\lambda = \frac{\lambda}{\lambda^{SM}}$$

- Measured **directly** with **Higgs boson pair (HH) production**

$$V \supset \frac{m_H^2}{2} H^2 + \lambda v H^3 + \frac{\lambda}{v} H^4$$

$$\lambda^{SM} = \frac{m_H^2}{2v^2} \sim 0.13$$

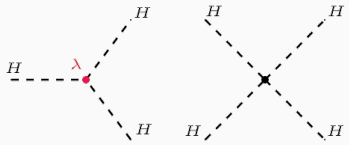

not accessible at LHC

Higgs boson self-coupling

$$V \supset \frac{m_H^2}{2} H^2 + \lambda v H^3 + \frac{\lambda}{v} H^4$$

$$\lambda^{SM} = \frac{m_H^2}{2v^2} \sim 0.13$$

- **Self-coupling:** **Higgs boson trilinear coupling**
- Controls the shape of the Higgs potential
  - It is important to measure both m_H and λ
- **B**eyond **SM** (BSM) physics would impact this coupling, impact quantified as

$$\kappa_\lambda = \frac{\lambda}{\lambda^{SM}}$$

- Measured **directly** with **Higgs boson pair (HH) production**

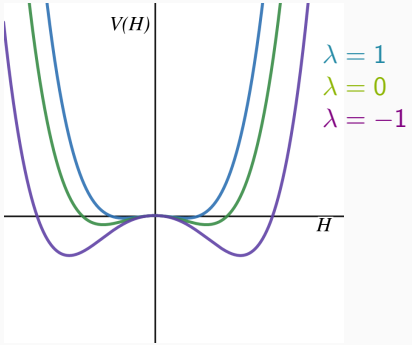

Higgs boson self-coupling

$$V \supset \frac{m_H^2}{2} H^2 + \lambda v H^3 + \frac{\lambda}{v} H^4$$

$$\lambda^{SM} = \frac{m_H^2}{2v^2} \sim 0.13$$

- **Self-coupling:** **Higgs boson trilinear coupling**
- Controls the shape of the Higgs potential
  - It is important to measure both m_H and λ
- **B**eyond **SM** (BSM) physics would impact this coupling, impact quantified as

$$\kappa_\lambda = \frac{\lambda}{\lambda^{SM}}$$

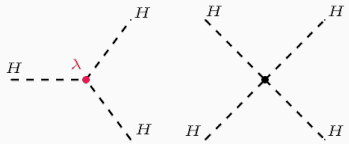

- Measured **directly** with **Higgs boson pair (HH) production**

Higgs boson pair production at the LHC

- Produced mainly via **non-resonant** **gluon-gluon Fusion (ggF)** and **Vector Boson Fusion (VBF)**

Destructive interference

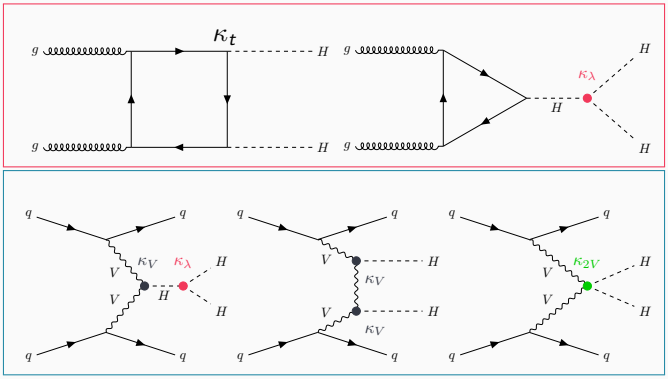

- At 13 TeV, $m_H = 125.09$ GeV and $\kappa_\lambda = 1$
  - $\sigma_{HH}^{ggF} = \mathbf{31.02\ fb}$, 3 order of magnitude smaller than σ_H
  - $\sigma_{HH}^{VBF} = \mathbf{1.72\ fb}$, one order of magnitude more smaller than ggF

Di-Higgs boson as a probe of BSM physics

- Low cross-section, BSM anomaly may enhance it
- BSM physics could manifest as deviations
  - **Total** production rate
  - **Kinematic** of HH event
- Measurement of $\kappa_\lambda \rightarrow \kappa_\lambda \neq \mathbf{1}$, presence of **new physics**

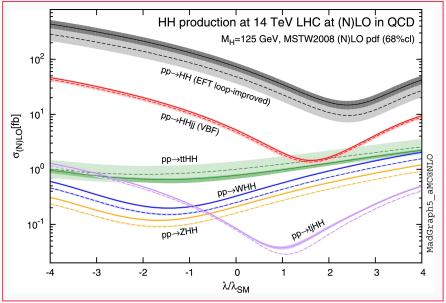

Di-Higgs boson as a probe of BSM physics

- Low cross-section, BSM anomaly may enhance it
- BSM physics could manifest as deviations
  - **Total** production rate
  - **Kinematic** of HH event
- Measurement of $\kappa_\lambda \rightarrow \kappa_\lambda \neq \mathbf{1}$, presence of **new physics**

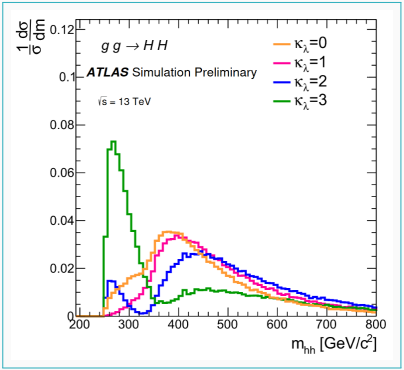

Di-Higgs boson decay modes

	bb	WW	$\tau\tau$	ZZ	$\gamma\gamma$
bb	**33%**				
WW	25%	4.6%			
$\tau\tau$	**7.4%**	2.5%	0.39%		
ZZ	3.1%	1.2%	0.34%	0.076%	
$\gamma\gamma$	**0.26%** ★	0.10%	0.029%	0.013%	0.0005%

- **Focusing on $H(\to b\bar{b})H(\to \gamma\gamma)$**
- Despite low decay rate, competitive channel
  - **High** $H\to b\bar{b}$ branching ratio
  - **Excellent** $m_{\gamma\gamma}$ mass resolution $\to$ **Good signal extraction**

Di-Higgs boson decay modes

	bb	WW	$\tau\tau$	ZZ	$\gamma\gamma$
bb	**33%**				
WW	25%	4.6%			
$\tau\tau$	**7.4%**	2.5%	0.39%		
ZZ	3.1%	1.2%	0.34%	0.076%	
$\gamma\gamma$	**0.26%** ★	0.10%	0.029%	0.013%	0.0005%

- **Focusing on $H(\rightarrow b\bar{b})H(\rightarrow \gamma\gamma)$**
- Despite low decay rate, competitive channel
  - **High** $H\rightarrow b\bar{b}$ branching ratio
  - **Excellent** $m_{\gamma\gamma}$ mass resolution $\rightarrow$ **Good signal extraction**

Content

The Large Hadron Collider (LHC)

- *pp* **collisions, up-to** $\sqrt{s} = 13$ **TeV**
- **Four large experiments**

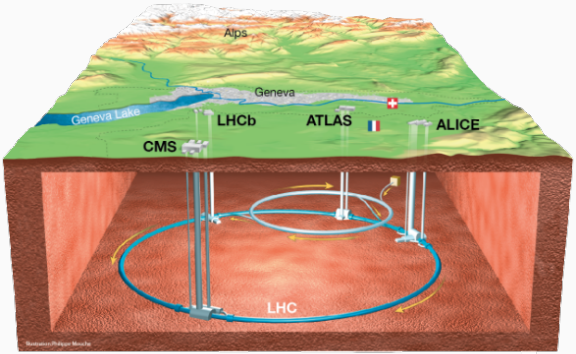

The ATLAS detector

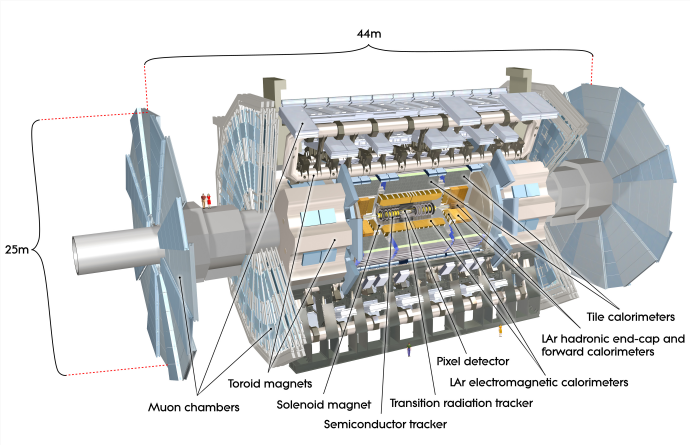

- **Different sub-detectors**
- **Cylindrical** coordinate system

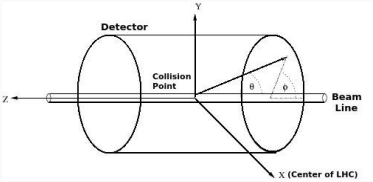

$$(p_T, \phi, \eta)$$

$$\eta = -\ln[\tan\frac{\theta}{2}]$$

Run-2 data taking

- Run-2 period: 2015-2018
- Integrated luminosity used for presented analysis: **139 fb^{-1}**

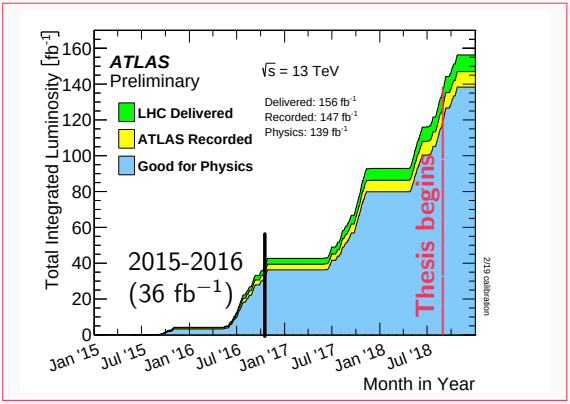

Where are we with HH$\to b\bar{b}\gamma\gamma$?

- Previous analysis: **2015-2016 data (36 fb^{-1})** **JHEP 11 (2018) 040**
  - $\frac{\sigma_{ggF}}{\sigma^{SM}}(HH)$ limit: **22** (Exp. **28**) at 95% CL
  - κ_λ constrain: **[-8.2, 13.2]** (Exp. **[-8.3, 13.2]**)
- My thesis: **Full run-2 data (139 fb^{-1})**
  - Improve the analysis sensitivity with different tools

	HH	HH$\to b\bar{b}\gamma\gamma$	$\sim$10% eff.
Events	4.3k	11	$\mathcal{O}(1)$

Where are we with HH$\to b\bar{b}\gamma\gamma$?

- Previous analysis: **2015-2016 data (36 fb^{-1})** **JHEP 11 (2018) 040**
  - $\frac{\sigma_{ggF}}{\sigma^{SM}}(HH)$ limit: **22** (Exp. **28**) at 95% CL
  - κ_λ constrain: **[-8.2, 13.2]** (Exp. **[-8.3, 13.2]**)
- My thesis: **Full run-2 data (139 fb^{-1})**
  - Improve the analysis sensitivity with different tools

	HH	HH$\to b\bar{b}\gamma\gamma$	$\sim$10% eff.
Events	4.3k	11	$\mathcal{O}(1)$

Content

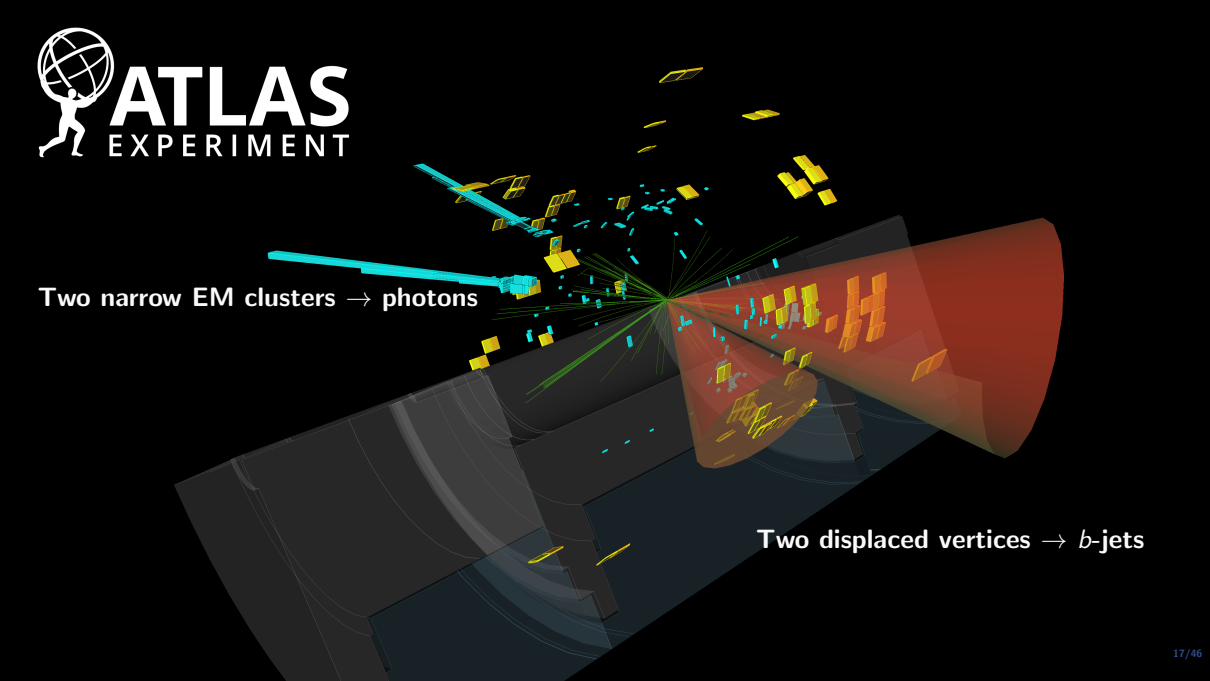
ATLAS
EXPERIMENT
Two narrow EM clusters → photons
Two displaced vertices → b-jets

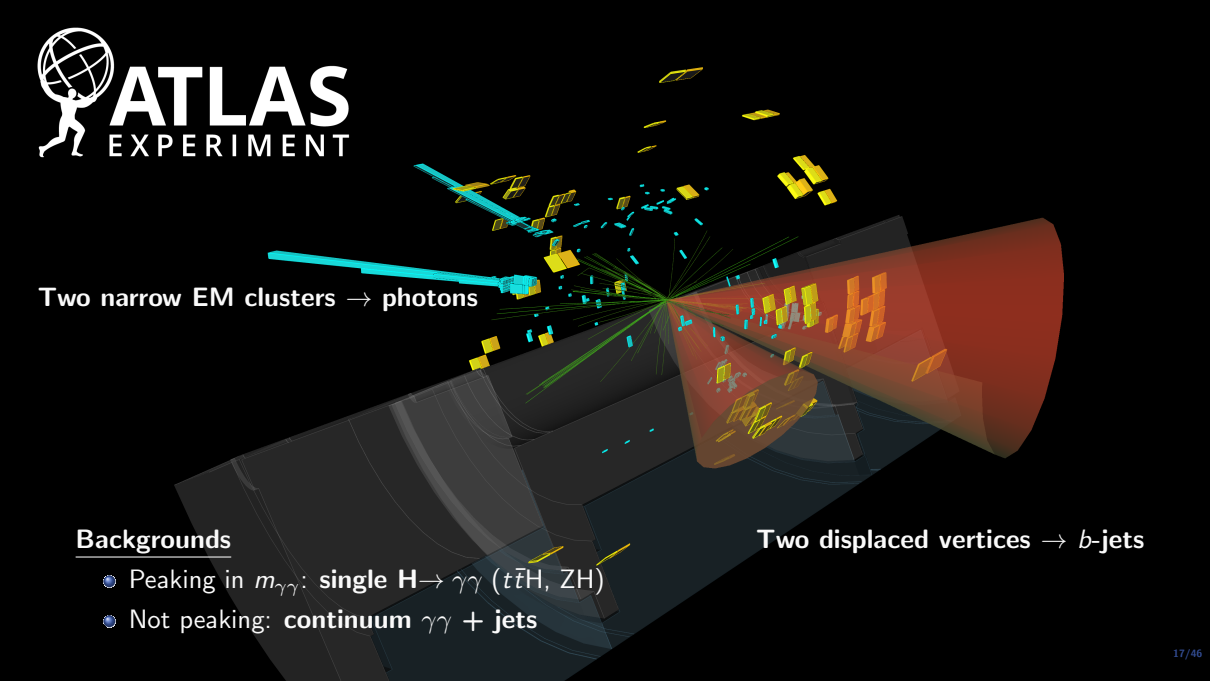

Backgrounds

- Peaking in $m_{\gamma\gamma}$: **single H**$\rightarrow \gamma\gamma$ ($t\bar{t}$H, ZH)
- Not peaking: **continuum** $\gamma\gamma$ **+ jets**

Events selection

- **Di-photon trigger** (83% efficiency for HH signal)
  - $E_T^{\gamma} > 35$ (25) GeV for leading (sub-leading)
- $\geq$ **2 Tight** and **isolated photons** (**H**$\rightarrow \gamma\gamma$)
  - $|\eta| < 2.37$ & $\frac{p_T^{\gamma}}{m_{\gamma\gamma}} > 35\%$ (25%) for leading (sub-leading)
  - $m_{\gamma\gamma}$ built with the two leading photons
- **Exactly 2** b**-jet** (**H**$\rightarrow b\bar{b}$)
  - $p_T > 25$ GeV & $|\eta| < 2.5$
  - b-tagging at 77% efficiency
- $<$ 6 jets, reject hadronic $t\bar{t}$H
- Zero leptons, reject semi-leptonic $t\bar{t}$H

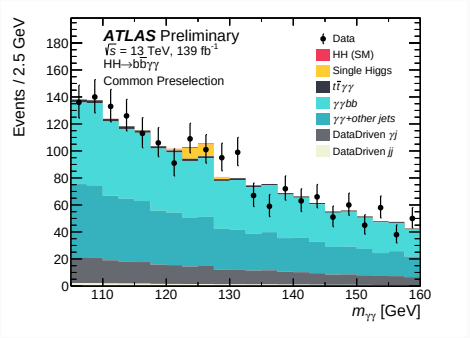

b-jet energy calibration

my own work

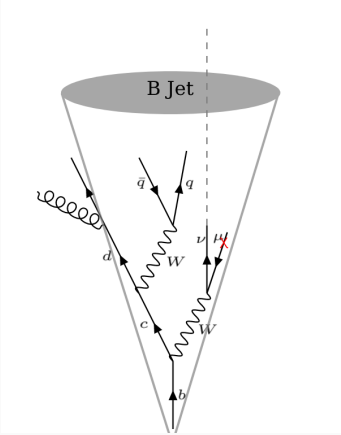

- $m_{b\bar{b}}$ highly discriminating for H$\rightarrow b\bar{b}$
- $\sigma_{m_{b\bar{b}}} \sim 16$ GeV, $\sigma_{m_{\gamma\gamma}} \sim 2$ GeV
- Jets energy calibration not enough for b-jets, due to
  - **Semi-leptonic** decay
  - **Large b-quark mass**
- Specific b-jet energy calibration method
  - μ**-in-jet correction**: presence of **muon**
  - p_T**Reco correction**: **missing neutrino** & **out-of-cone** radiation

b-jet energy calibration

my own work

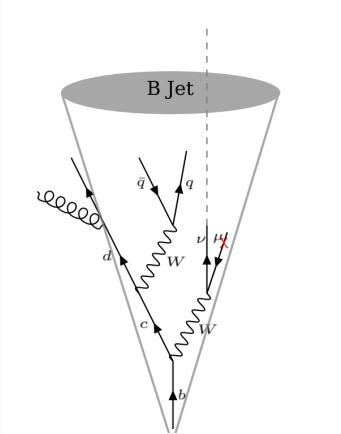

- $m_{b\bar{b}}$ highly discriminating for H$\rightarrow b\bar{b}$
- $\sigma_{m_{b\bar{b}}} \sim 16$ GeV, $\sigma_{m_{\gamma\gamma}} \sim 2$ GeV
- Jets energy calibration not enough for b-jets, due to
  - **Semi-leptonic** decay
  - **Large b-quark mass**
- Specific b-jet energy calibration method
  - **μ-in-jet correction**: presence of **muon**
  - **p_TReco correction**: **missing neutrino** & **out-of-cone** radiation

b-jet energy calibration

my own work

- μ-**in-jet** correction
  - Adding back muons
  - Variable ΔR(b-jet, muon)
  - Semi-leptonic or hadronic
- p_T**Reco** correction
  - p_T-dependent scale factor
  - Computed on $t\bar{t}$ **sample**

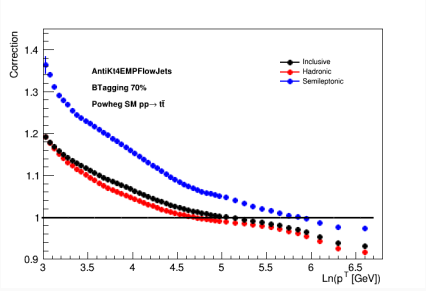

b-jet energy calibration

my own work

- μ-**in-jet** correction
  - Adding back muons
  - Variable ΔR(b-jet, muon)
  - Semi-leptonic or hadronic
- p_T**Reco** correction
  - p_T-dependent scale factor
  - Computed on $t\bar{t}$ **sample**

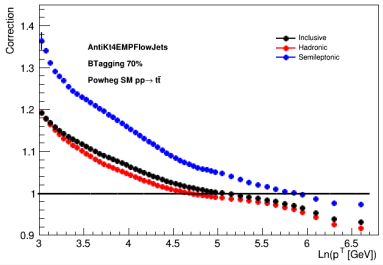

- Applied to HH→ $b\bar{b}\gamma\gamma$ b-jets

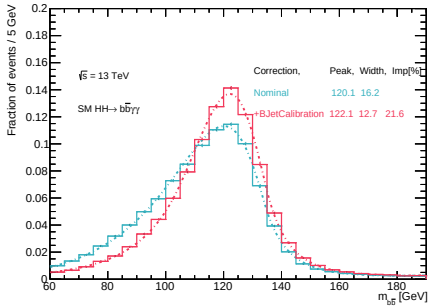

- ∼**22%** imp. on $m_{b\bar{b}}$ resolution
- **7%** $\pm$ **2%** imp. on expected significance
- **Baseline** b-**jet correction** *for full Run-2 HH search*

Categorization strategy

- Sensitivity to
  - **SM HH signal**
  - κ_λ **deviations**
- Two mass regions on $m^*_{b\bar{b}\gamma\gamma}$
  - **High mass** $m^*_{b\bar{b}\gamma\gamma} > 350$ **GeV**
  - **Low mass** $m^*_{b\bar{b}\gamma\gamma} < 350$ **GeV**
- Signal-background separation: **MVA**

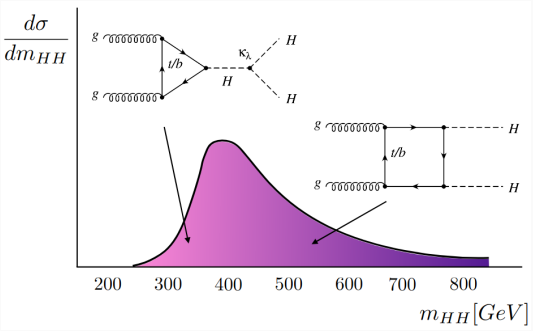

Categorization strategy

- Sensitivity to
  - **SM HH signal**
  - κ_λ **deviations**
- Two mass regions on $m^*_{b\bar{b}\gamma\gamma}$
  - **High mass** $m^*_{b\bar{b}\gamma\gamma} > 350$ **GeV**
  - **Low mass** $m^*_{b\bar{b}\gamma\gamma} < 350$ **GeV**
- Signal-background separation: **MVA**

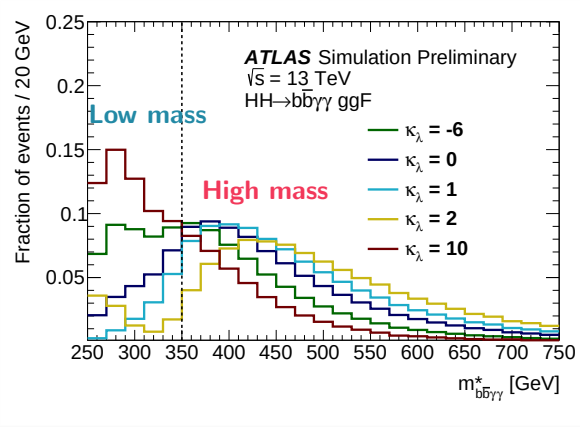

$$m^*_{b\bar{b}\gamma\gamma} = m_{b\bar{b}\gamma\gamma} - m_{b\bar{b}} - m_{\gamma\gamma} + 250 \text{ GeV}$$

MVA categorization

- Two MVA are trained to discriminate signal from the backgrounds
  - **High mass**: **SM HH** ($\kappa_\lambda = 1$)
  - **Low mass**: **BSM HH** ($\kappa_\lambda = 10$)
- Same inputs: objects and event kinematic
- MVA techniques
  - **B**oosted **D**ecision **T**rees: signal vs ($t\bar{t}$H + ZH + continuum $\gamma\gamma$ + jets)
  - **D**eep **N**eural **N**etwork: signal vs $t\bar{t}$H vs ZH vs continuum $\gamma\gamma$ + jets

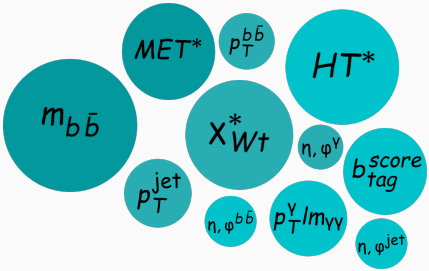

* not used in DNN

Deep Neural Network selection

my own work

- d_{HH} discriminate from 4 probabilities:

$$d_{HH} = \log\left(\frac{\sigma_{HH} \cdot p_{HH}}{\sum^{3} \sigma_{bkg} \cdot p_{bkg}}\right)$$

- **4 categories** maximize combined expected significance
  - **tight** and **loose** DNN for each mass region
- Similar performance to the BDT
- Baseline: **BDT**
- **DNN** *reserved and documented for next analysis round*

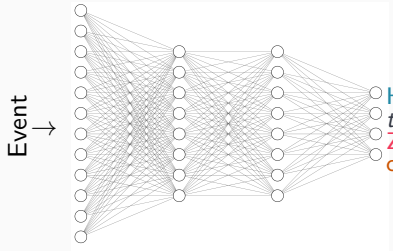

MVA	SM HH	HH $\kappa_\lambda = 10$
BDT	0.49σ	3.59σ
DNN	0.54σ	3.47σ

$$\text{significance} = \sqrt{2[(s+b) \times \log(1+s/b) - s]}$$

Deep Neural Network selection

my own work

- d_{HH} discriminate from 4 probabilities:

$$d_{HH} = \log\left(\frac{\sigma_{HH} \cdot p_{HH}}{\sum^{3} \sigma_{bkg} \cdot p_{bkg}}\right)$$

- **4 categories** maximize combined expected significance
  - **tight** and **loose** DNN for each mass region
- Similar performance to the BDT
- Baseline: BDT
- **DNN** *reserved and documented for next analysis round*

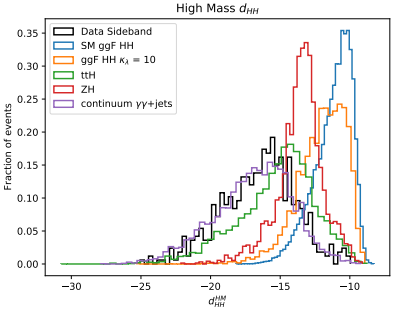

MVA	SM HH	HH $\kappa_\lambda = 10$
BDT	0.49σ	3.59σ
DNN	0.54σ	3.47σ

$$\text{significance} = \sqrt{2[(s+b) \times \log(1 + s/b) - s]}$$

Deep Neural Network selection

my own work

- d_{HH} discriminate from 4 probabilities:

$$d_{HH} = \log\left(\frac{\sigma_{HH} \cdot p_{HH}}{\sum^{3} \sigma_{bkg} \cdot p_{bkg}}\right)$$

- **4 categories** maximize combined expected significance
  - **tight** and **loose** DNN for each mass region
- **Similar performance to the BDT**
- Baseline: **BDT**
- **DNN** *reserved and documented for next analysis round*

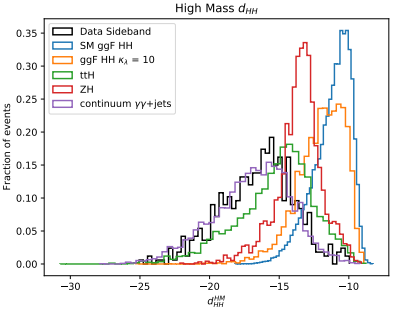

MVA	SM HH	HH $\kappa_\lambda = 10$
BDT	0.49σ	3.59σ
DNN	0.54σ	3.47σ

$$\text{significance} = \sqrt{2[(s+b) \times \log(1 + s/b) - s]}$$

Deep Neural Network selection

my own work

- d_{HH} discriminate from 4 probabilities:

$$d_{HH} = \log\left(\frac{\sigma_{HH} \cdot p_{HH}}{\sum^{3} \sigma_{bkg} \cdot p_{bkg}}\right)$$

- **4 categories** maximize combined expected significance
  - **tight** and **loose** DNN for each mass region
- **Similar performance to the BDT**
- Baseline: **BDT**
- **DNN** *reserved and documented for next analysis round*

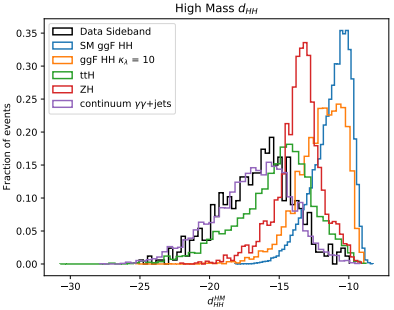

MVA	SM HH	HH $\kappa_\lambda = 10$
BDT	0.49σ	3.59σ
DNN	0.54σ	3.47σ

$$\text{significance} = \sqrt{2[(s+b) \times \log(1+s/b) - s]}$$

Signal extraction and results

- Simultaneous fit of $m_{\gamma\gamma}$ in the 4 analysis categories
  - **HH signal (ggF + VBF)** + **Single Higgs**
    - **from Monte Carlo** using Double-sided Crystal-Ball
  - **Continuum $\gamma\gamma$ + jets**
    - **fully data driven**
- **No significant signal is observed**
- 95% CL upper limits on $\sigma_{ggF+VBF}$ of diHiggs as a function of κ_λ

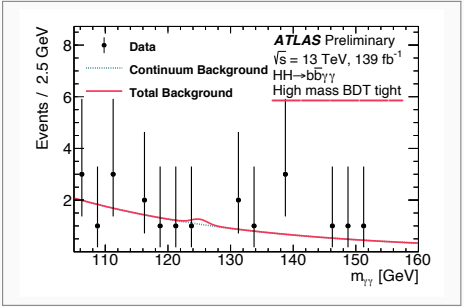

most sensitive category

Limits and κ_λ constrain

ATLAS-CONF-2021-016

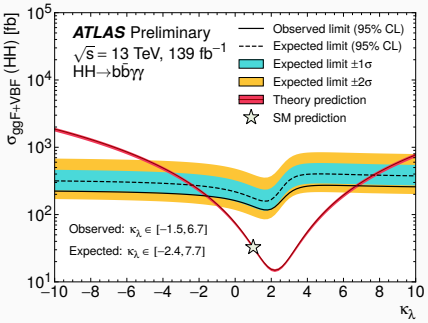

- $\frac{\sigma_{HH}}{\sigma_{HH}^{SM}}$ limit: **4.1** (Exp. **5.5**) at 95% CL
- κ_λ constrain: **[-1.5, 6.7]** (Exp. **[-2.4, 7.7]**)
- **Statistically limited**
  - Systematic effect $\sim$ **4%**
  - Background modelling & photon energy scale

Limits and κ_λ constrain

ATLAS-CONF-2021-016

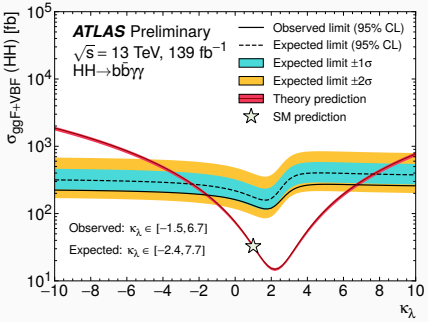

- $\frac{\sigma_{HH}}{\sigma_{HH}^{SM}}$ limit: **4.1** (Exp. **5.5**) at 95% CL
- κ_λ constrain: **[-1.5, 6.7]** (Exp. **[-2.4, 7.7]**)
- **Statistically limited**
  - Systematic effect $\sim$ **4%**
  - Background modelling & photon energy scale
- **5× improvement** w.r.t 36 fb^{-1}
  - Increased luminosity: 2×
  - **Analysis improvement: almost 3×**
    - m_{HH} categorization and MVA strategy (**80%**)
    - b-jet energy calibration (**7%**)
    - ...

The world's best κ_λ limit

Limits and κ_λ constrain

ATLAS-CONF-2021-016

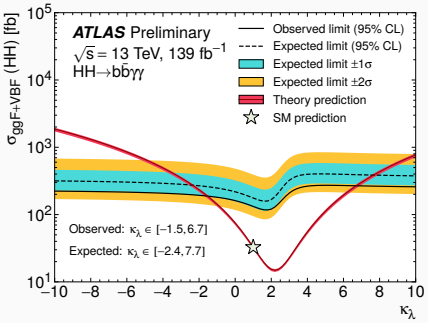

- $\frac{\sigma_{HH}}{\sigma_{HH}^{SM}}$ limit: **4.1** (Exp. **5.5**) at 95% CL
- κ_λ constrain: **[-1.5, 6.7]** (Exp. **[-2.4, 7.7]**)
- **Statistically limited**
  - Systematic effect $\sim$ **4%**
  - Background modelling & photon energy scale
- **5× improvement** w.r.t 36 fb^{-1}
  - Increased luminosity: 2×
  - **Analysis improvement: almost 3×**
    - m_{HH} categorization and MVA strategy (**80%**)
    - b-jet energy calibration (**7%**)
    - ...

Limits and κ_λ constrain

ATLAS-CONF-2021-016

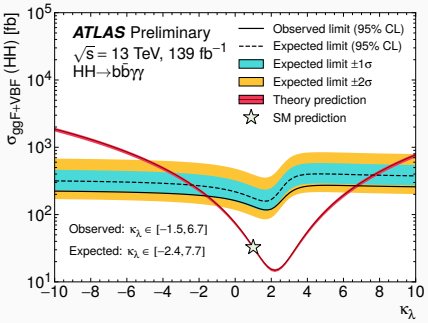

- $\frac{\sigma_{HH}}{\sigma_{HH}^{SM}}$ limit: **4.1** (Exp. **5.5**) at 95% CL
- κ_λ constrain: **[-1.5, 6.7]** (Exp. **[-2.4, 7.7]**)
- **Statistically limited**
  - Systematic effect $\sim$ **4%**
  - Background modelling & photon energy scale
- **5× improvement** w.r.t 36 fb^{-1}
  - Increased luminosity: 2×
  - **Analysis improvement: almost 3×**
    - m_{HH} categorization and MVA strategy (**80%**)
    - b-jet energy calibration (**7%**)
    - ...

CMS HH$\rightarrow b\bar{b}\gamma\gamma$ results

JHEP03 (2021) 257

- **Different analysis strategies**
  - 14 categories
    - **MVAs output** and $m^{*}_{b\bar{b}\gamma\gamma}$
    - **2 dedicated VBF categories**
  - **2D fit** $m_{\gamma\gamma} \times m_{b\bar{b}}$

	Expected	Observed
CMS $\frac{\sigma_{HH}}{\sigma^{SM}_{HH}}$ limit	**5.2**	7.7
CMS κ_λ interval	**[-2.5, 8.2]**	[-3.3, 8.5]
ATLAS $\frac{\sigma_{HH}}{\sigma^{SM}_{HH}}$ limit	**5.5**	4.1
ATLAS κ_λ interval	**[-2.4, 7.7]**	[-1.5, 6.7]

Content

Effective Field Theory (EFT)

- Search for new physics at large energy scale (Λ) in a **model independent** way
- At large scale ($\Lambda >> v$), BSM decouples from SM

$$\mathcal{L} = \mathcal{L}_{SM} + \mathcal{L}^5 + \mathcal{L}^6 + \mathcal{L}^7 + \ldots, \quad \mathcal{L}^d = \sum_{i=1}^{n_d} \frac{c_i^d}{\Lambda^{d-4}} \mathcal{O}_i^d \quad \text{for } d > 4$$

- **Cross-section** (and **decay width**) can be split

$$\sigma = \sigma_{SM} + \sigma_{int} + \sigma_{BSM}$$

$$\frac{\sigma}{\sigma_{SM}} = 1 + \sum_i a_i \cdot c_i + \sum_{i,j} b_{ij} \cdot c_i \cdot c_j$$

- **Standard Model Effective Field Theory** (SMEFT) in **Warsaw** basis with $\mathbf{d = 6}$ and $\Lambda = \mathbf{1\ TeV}$

Di-Higgs and EFT

- 5 operators are relevant for di-Higgs
  - c_H and $c_{H\Box}$ modify the Higgs self-coupling κ_λ

$$\kappa_\lambda = 1 - 2\frac{v^4}{m_H^2} \cdot c_H + 3\left(c_{H\Box} - \frac{c_{HD}}{4}\right)$$

  - c_{uH} and c_{tG} modify the top quark interaction to the Higgs and gluons.

$$\kappa_t = 1 + \left(c_{H\Box} - \frac{c_{HD}}{4}\right) - \frac{v^3}{\sqrt{2}m_t} \cdot c_{uH}$$

  - c_{HG}, modify the Higgs coupling to gluons (**not considered**).

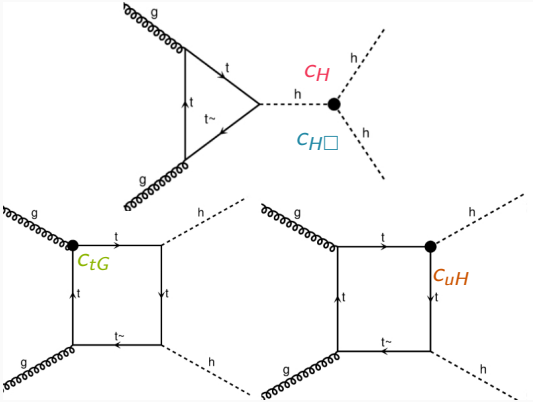

Di-Higgs and EFT

- 5 operators are relevant for di-Higgs
  - c_H and $c_{H\Box}$ modify the Higgs self-coupling κ_λ

$$\kappa_\lambda = 1 - 2\frac{v^4}{m_H^2} \cdot c_H + 3\left(c_{H\Box} - \frac{c_{HD}}{4}\right)$$

  - c_{uH} and c_{tG} modify the top quark interaction to the Higgs and gluons.

$$\kappa_t = 1 + \left(c_{H\Box} - \frac{c_{HD}}{4}\right) - \frac{v^3}{\sqrt{2}m_t} \cdot c_{uH}$$

  - c_{HG}, modify the Higgs coupling to gluons (**not considered**).

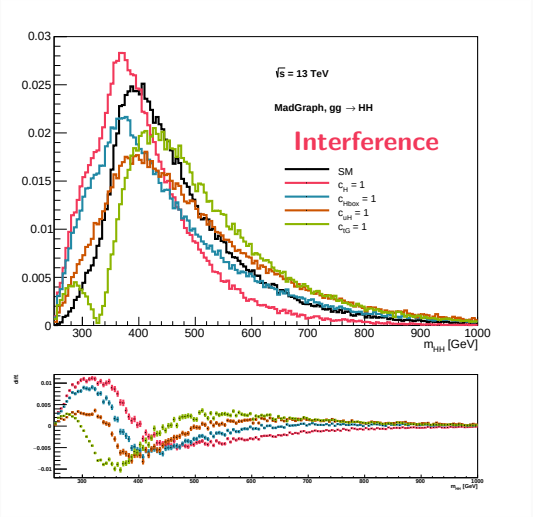

Cross-section parameterization in HH $\rightarrow b\bar{b}\gamma\gamma$

my own work

- $b\bar{b}\gamma\gamma$ measurements in two phase space regions
  - **High mass** ($m_{HH} > 350$ GeV)
  - **Low mass** ($m_{HH} < 350$ GeV)
- ggF HH cross-section parameterized as function of the Wilson coefficients

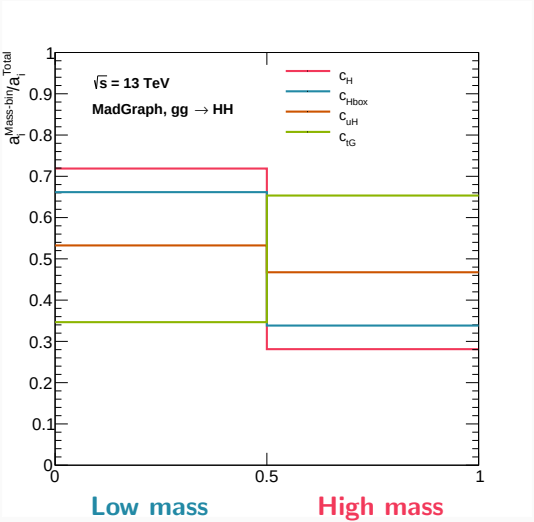

Results

- Not sensitive to all coefficients (**two mass regions**)
  → Need **sensitivity estimate** to find relevant ones
  - Look at the eigenvectors of the inverse covariance matrix of Wilson coefficients

	Eigenvalue	Eigenvector
vec_0	0.0523	$- 0.582 \cdot c_H + 0.363 \cdot c_{H\Box} - 0.456 \cdot c_{uH} + 0.567 \cdot c_{tG}$
vec_1	0.0001	$- 0.696 \cdot c_H + 0.182 \cdot c_{H\Box} + 0.206 \cdot c_{uH} - 0.663 \cdot c_{tG}$
vec_3	-0.0000	$- 1.025 \cdot c_H - 1.947 \cdot c_{H\Box} + 0.702 \cdot c_{uH} + 0.759 \cdot c_{tG}$
vec_4	-0.0000	$- 0.235 \cdot c_H - 0.006 \cdot c_{H\Box} + 0.977 \cdot c_{uH} + 0.549 \cdot c_{tG}$

- Measurement of most sensitive eigenvectors

	expected error
vec_0	$^{+3.9}_{5.1}$
vec_1	$^{+80.8}_{-102.1}$

- Additional measurement regions, combination with other measurements (Higgs, Top) needed
- **Work in progress**

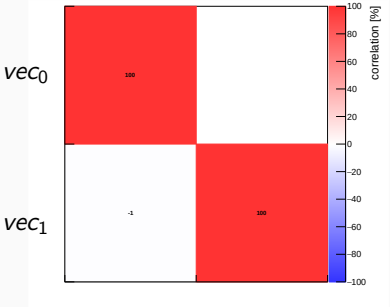

Content

Prospects at the end of Run-3

my own work

- **Run-2+Run-3**: $\mathcal{L}_{int} \sim 300$ fb^{-1}, $\sqrt{s} = 13.6$ TeV
  - Detector upgrades: **no significant impact on HH**$\rightarrow b\bar{b}\gamma\gamma$
- $\frac{\sigma_{HH}}{\sigma_{HH}^{SM}}$ limit: **3.3** (**1.6**$\times$ **imp.** w.r.t 139 fb^{-1})

Scenario	1σ CI	2σ CI
Run-2	[-1.3, 6.4]	[-2.9, 8]
Run-2+Run-3	**[-0.7, 5.6]**	**[-1.9, 7]**

Potential improvements:

- **DNN categorization**: $\sim$**10%**
- $m_{b\bar{b}}$ imp. with **kinematic fit**: **2-5%**
- **Photon identification**: **7%** (next part)

Prospects at the end of Run-3

my own work

- **Run-2+Run-3**: $\mathcal{L}_{int} \sim 300$ fb^{-1}, $\sqrt{s} = 13.6$ TeV
  - Detector upgrades: **no significant impact on HH**$\rightarrow b\bar{b}\gamma\gamma$
- $\frac{\sigma_{HH}}{\sigma_{HH}^{SM}}$ limit: **3.3** (**1.6**$\times$ **imp.** w.r.t 139 fb^{-1})

Scenario	1σ CI	2σ CI
Run-2	[-1.3, 6.4]	[-2.9, 8]
Run-2+Run-3	**[-0.7, 5.6]**	**[-1.9, 7]**

Potential improvements:

- **DNN categorization**: ~10%
- $m_{b\bar{b}}$ imp. with **kinematic fit**: 2-5%
- **Photon identification**: 7% (next part)

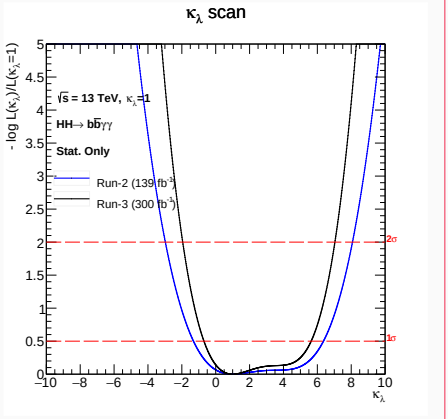

Prospects at the end of Run-3

my own work

- **Run-2+Run-3**: $\mathcal{L}_{int} \sim 300$ fb^{-1}, $\sqrt{s} = 13.6$ TeV
  - Detector upgrades: **no significant impact on HH$\rightarrow b\bar{b}\gamma\gamma$**
- $\frac{\sigma_{HH}}{\sigma_{HH}^{SM}}$ limit: **3.3** (**1.6$\times$ imp.** w.r.t 139 fb^{-1})

Scenario	1σ CI	2σ CI
Run-2	[-1.3, 6.4]	[-2.9, 8]
Run-2+Run-3	**[-0.7, 5.6]**	**[-1.9, 7]**

Potential improvements:

- **DNN categorization**: $\sim$**10%**
- $m_{b\bar{b}}$ imp. with **kinematic fit**: **2-5%**
- **Photon identification**: **7%** (next part)

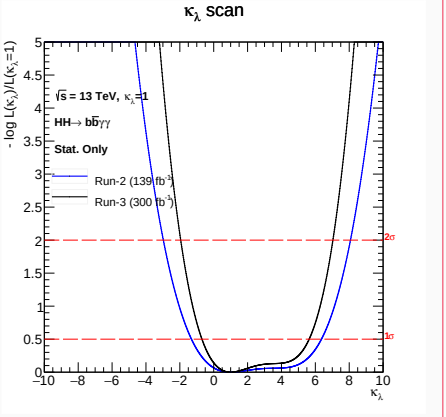

Prospects at HL-LHC

my own work

- **HL-LHC: $\sim$3000 fb^{-1} at 14 TeV**
- Detector upgrades: **mitigate higher pileup effects**
- European strategy: extrapolation from 36 fb^{-1}

Scenario	1σ CI	2σ CI
European strategy	[-0.1, 2.4]	[-1.1, 8.1]
My Extra. to HL-LHC	**[0.4, 1.8]**	**[-0.1, 4.4]**

Prospects at HL-LHC

my own work

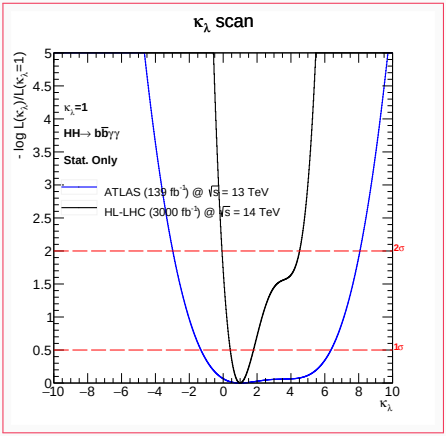

- **HL-LHC: ∼3000 fb^{-1} at 14 TeV**
- Detector upgrades: **mitigate higher pileup effects**
- European strategy: extrapolation from 36 fb^{-1}

Scenario	1σ CI	2σ CI
European strategy	[-0.1, 2.4]	[-1.1, 8.1]
My Extra. to HL-LHC	**[0.4, 1.8]**	**[-0.1, 4.4]**

Prospects at HL-LHC

my own work

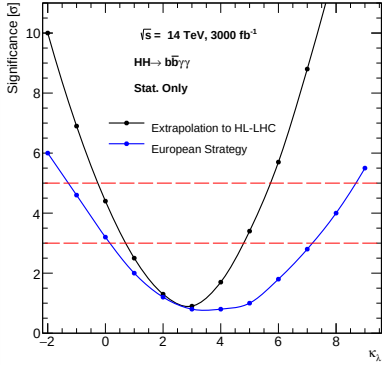

- **HL-LHC:** $\sim$3000 fb^{-1} **at** 14 TeV
- Detector upgrades: **mitigate higher pileup effects**
- European strategy: extrapolation from 36 fb^{-1}

Scenario	Significance [σ]
European strategy	2.1
My Extra. to HL-LHC	**2.5**

Similar performances for SM
Large gain at high κ_λ

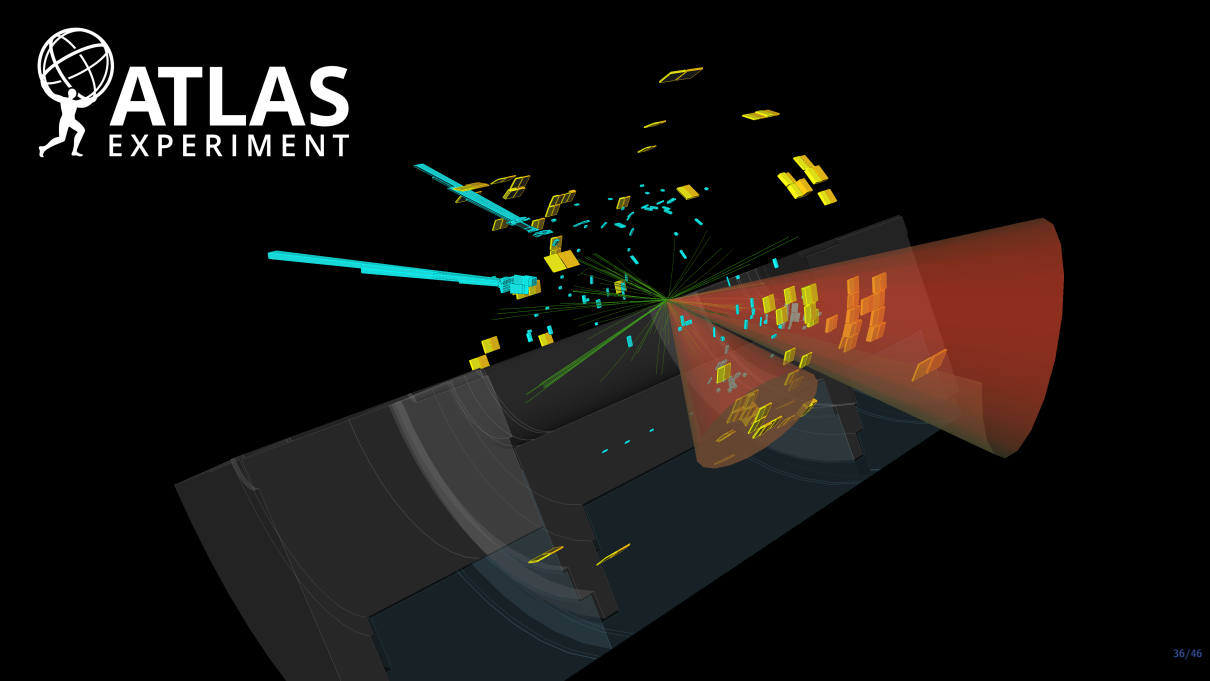
ATLAS
EXPERIMENT

Content

EM calorimeter and γ object

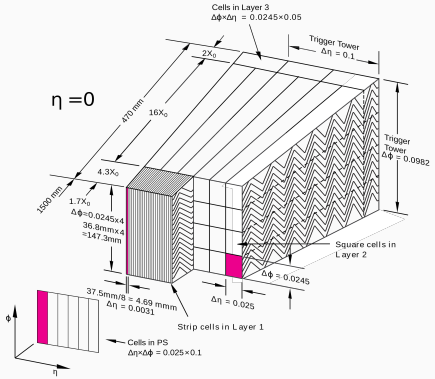

- **3 layers** with different **cell size** (+ Presampler)
- $N_\eta \times N_\phi$ **cluster** contains most γ energy
- **Shower shapes** (SS) quantities ($\sim$ 11) evaluated from 7×11 cluster
  - **Lateral** & **longitudinal** EM shower
  - **Discriminate between prompt photons and background photons** (QCD jets)
- Current identification relies on SS: **cut-based algorithm**
- **Propose improvement using Neural Network**

EM calorimeter and γ object

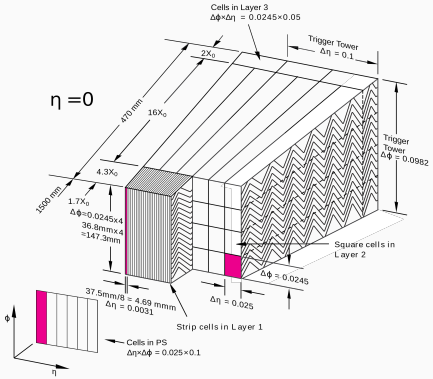

- **3 layers** with different **cell size** (+ Presampler)
- $N_\eta \times N_\phi$ **cluster** contains most γ energy
- **Shower shapes** (SS) quantities ($\sim$ 11) evaluated from 7×11 cluster
  - **Lateral** & **longitudinal** EM shower
  - **Discriminate between prompt photons and background photons** (QCD jets)

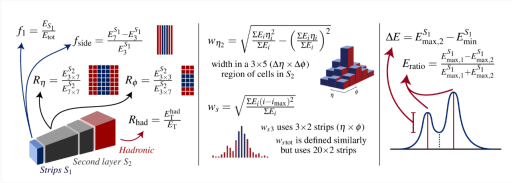

- Current identification relies on SS: **cut-based algorithm**
- **Propose improvement using Neural Network**

EM calorimeter and γ object

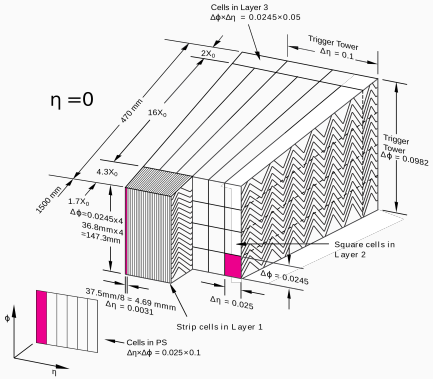

- **3 layers** with different **cell size** (+ Presampler)
- $N_\eta \times N_\phi$ **cluster** contains most γ energy
- **Shower shapes** (SS) quantities ($\sim$ 11) evaluated from 7×11 cluster
  - **Lateral** & **longitudinal** EM shower
  - **Discriminate between prompt photons and background photons** (QCD jets)

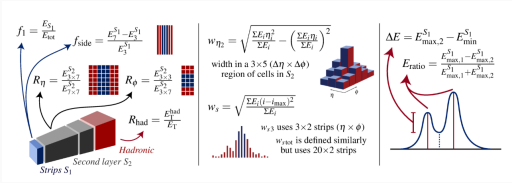

- Current identification relies on SS: **cut-based algorithm**
- **Propose improvement using Neural Network**

Photon identification with Neural Network

- Global shower shapes (High level)
  Cut-based $\rightarrow$ DNN
  - **Limited performance** (small features space)
- Solution: **breakdown to cell level** (Low level)
  - Scale up features space dimensionality
    - **Generate more variables**
    - **Correlation between cells**
- **Convolutional Neural Network (CNN)**
  - Photon cluster represented as an image
- Photon identification (ID) using images from the 3 layers

Photon identification with Neural Network

- Global shower shapes (High level)
  Cut-based → DNN
  - **Limited performance** (small features space)
- Solution: **breakdown to cell level** (Low level)
  - Scale up features space dimensionality
    - **Generate more variables**
    - **Correlation between cells**
- **Convolutional Neural Network (CNN)**
  - Photon cluster represented as an image
- Photon identification (ID) using images from the 3 layers

Photon identification with Neural Network

- Global shower shapes (High level)
  Cut-based → DNN
  - **Limited performance** (small features space)
- Solution: **breakdown to cell level** (Low level)
  - Scale up features space dimensionality
    - **Generate more variables**
    - **Correlation between cells**
- **Convolutional Neural Network (CNN)**
  - Photon cluster represented as an image
- Photon identification (ID) using images from the 3 layers

7×11 cluster from 2^{nd} layer

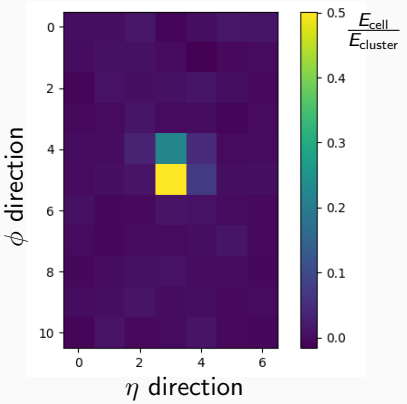

Convolutional Neural Network strategy and training

my own work

- **Prompt photons**: inclusive γ+jets events
- **Background photons**: QCD di-jet events
- Images from **7×11 windows**
  - **Energy independent algorithm**
  - Image pixel = cell energy fraction
- **Inclusive training** (E_T, $|\eta| < 2.4$, conversion type)
- **Trained on Monte Carlo**
- CNN **over-performs** the cut-based algorithm

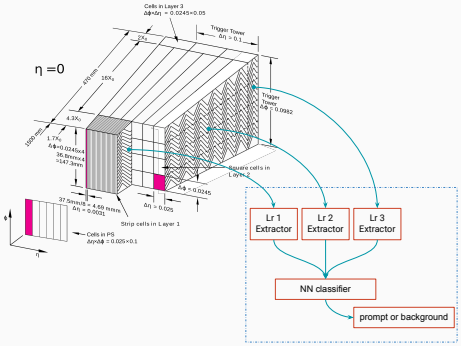

Convolutional Neural Network strategy and training

my own work

- **Prompt photons**: inclusive γ+jets events
- **Background photons**: QCD di-jet events
- Images from **7×11 windows**
  - **Energy independent algorithm**
  - Image pixel = cell energy fraction
- **Inclusive training** (E_T, $|\eta| < 2.4$, conversion type)
- **Trained on Monte Carlo**
- CNN **over-performs** the cut-based algorithm

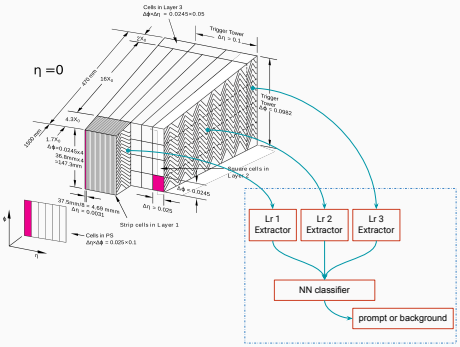

Convolutional Neural Network strategy and training

my own work

- **Prompt photons**: inclusive γ+jets events
- **Background photons**: QCD di-jet events
- Images from **7×11 windows**
  - **Energy independent algorithm**
  - Image pixel = cell energy fraction
- **Inclusive training** (E_T, $|\eta| < 2.4$, conversion type)
- **Trained on Monte Carlo**
- CNN **over-performs** the cut-based algorithm

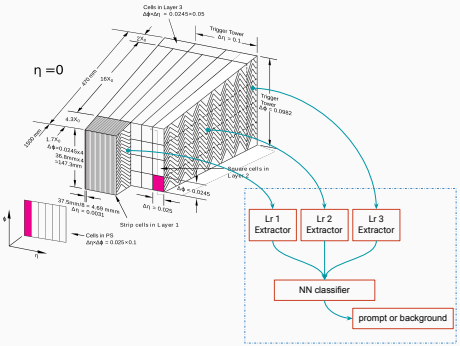

Convolutional Neural Network strategy and training

my own work

- **Prompt photons**: inclusive γ+jets events
- **Background photons**: QCD di-jet events
- Images from **7×11 windows**
  - **Energy independent algorithm**
  - Image pixel = cell energy fraction
- **Inclusive training** (E_T, $|\eta| < 2.4$, conversion type)
- **Trained on Monte Carlo**
- CNN **over-performs** the cut-based algorithm

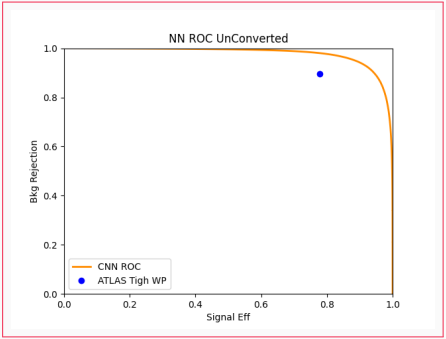

Photon identification efficiency

my own work

- Identification efficiency with **Radiative Z method**
  - $Z \to ll\gamma$ (l=e,μ), **as a signal**
  - $Z \to ll$+jet (l=e,μ), **as a background**
  - **2017 data** (43.6 fb^{-1})
- Efficiency as

$$\epsilon_{ID} = \frac{N^{\text{after ID}} \times P^{\text{after ID}}}{N^{\text{before ID}} \times P^{\text{before ID}}}$$

- Purity estimated with **template fit of** $m_{ll\gamma}$
- **Over-performs** the cut-based algorithm
  - Out-of-sample validation: **different event topology**
  - **Good data-MC agreement**

Photon identification efficiency

my own work

- Identification efficiency with **Radiative Z method**
  - $Z \to ll\gamma$ (l=e,μ), **as a signal**
  - $Z \to ll$+jet (l=e,μ), **as a background**
  - **2017 data** (43.6 fb^{-1})
- Efficiency as

$$\epsilon_{ID} = \frac{N^{\text{after ID}} \times P^{\text{after ID}}}{N^{\text{before ID}} \times P^{\text{before ID}}}$$

- Purity estimated with **template fit of** $m_{ll\gamma}$
- **Over-performs** the cut-based algorithm
  - Out-of-sample validation: **different event topology**
  - **Good data-MC agreement**

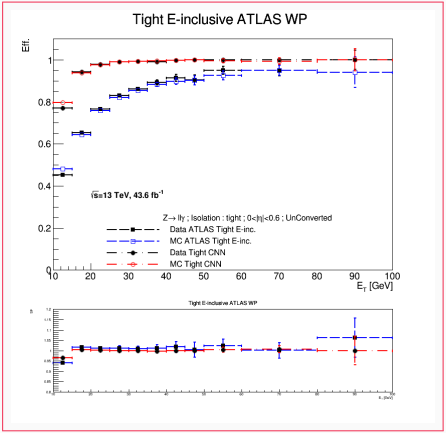

Impact on HH$\rightarrow b\bar{b}\gamma\gamma$ analysis

my own work

- CNN applied to photons from HH$\rightarrow b\bar{b}\gamma\gamma$ signal
  - **Efficiency close to 100%**
  - **15% improvement in signal acceptance**
- CNN applied to photons from continuum $\gamma\gamma$+jets
  - **high $\gamma\gamma$ purity**
  - **15% increase in statistics**
  - **Reduce background modelling systematics**
- $\sim$ **7.3% improvement in analysis significance**

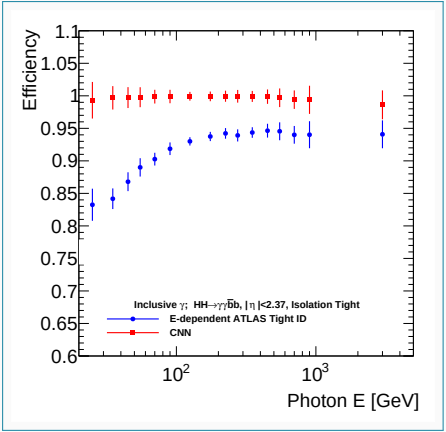

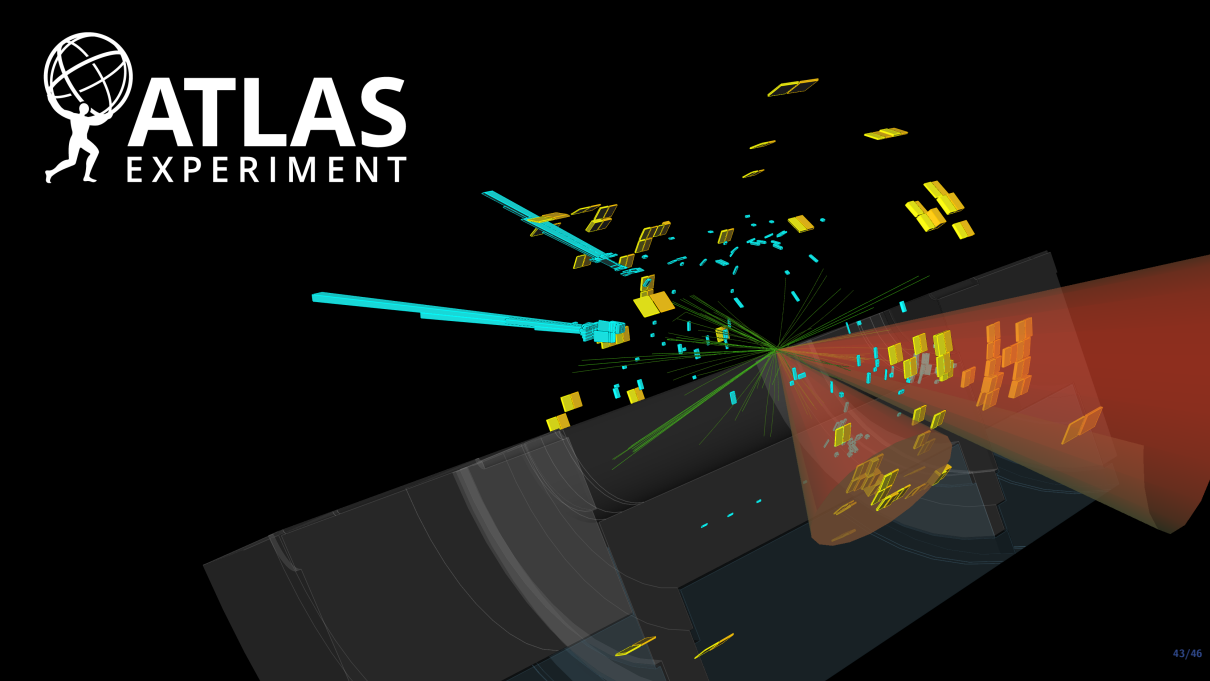
ATLAS
EXPERIMENT

Conclusion

- **Search for non-resonant HH production and measurement of Higgs self-coupling**
  - **HH$\rightarrow b\bar{b}\gamma\gamma$ golden channel $\rightarrow$ The world's best κ_λ limit**
  - **Re-interpretation** within EFT context
  - **Extrapolation** to Run-3 and to HL-LHC
- **New Photon identification using Convolutional Neural Network**
  - **Significance improvement** in different events topologies
  - **Relevant** for HH$\rightarrow b\bar{b}\gamma\gamma$ in future
- **Work not presented**
  - **Kinematic Fit** for HH$\rightarrow b\bar{b}\gamma\gamma$
  - **Shower shape mis-modelling** correction
- **Parallel work**
  - **96 hours of lab work** at the Savoie Mont Blanc University

Thank you for your attention

Big thanks to all the people with whom I had the chance to work during my PhD

BACKUP

Higgs production modes

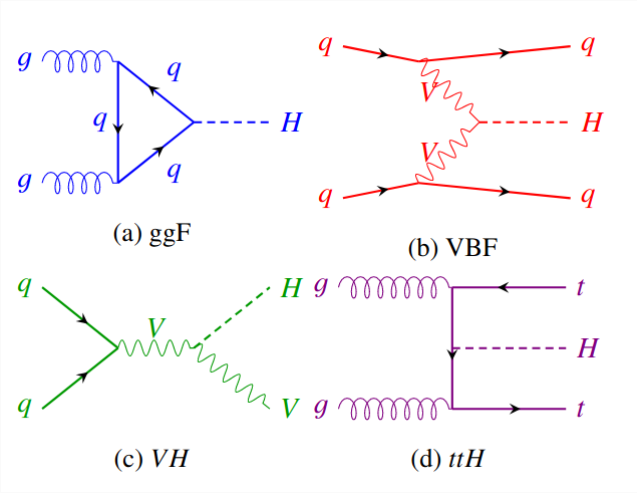

Higgs cross-section

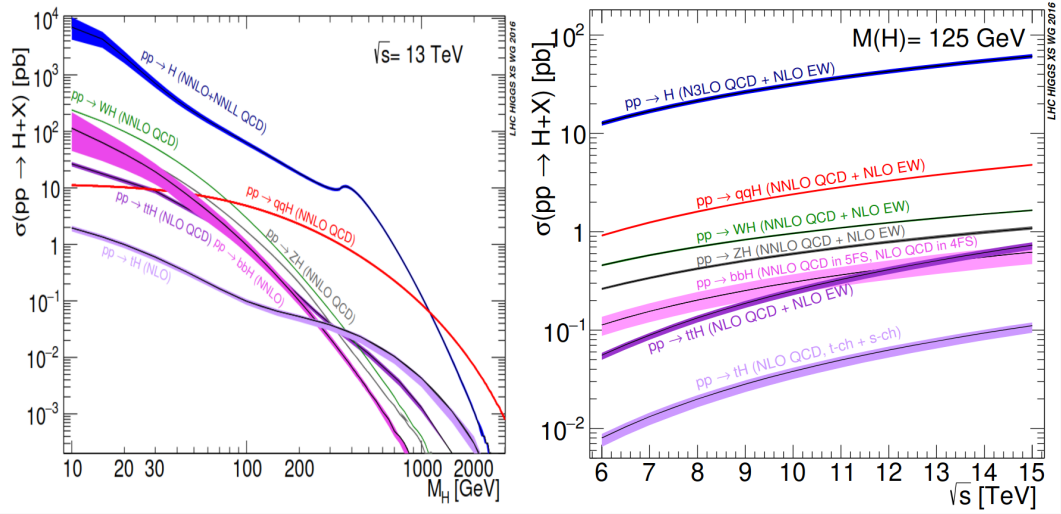

Higgs decay modes

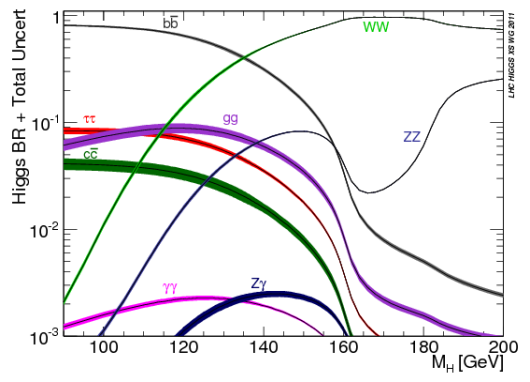

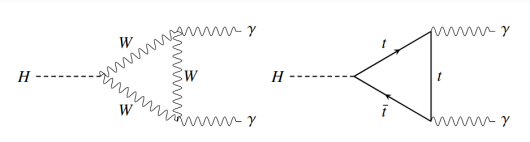

Higgs self-coupling

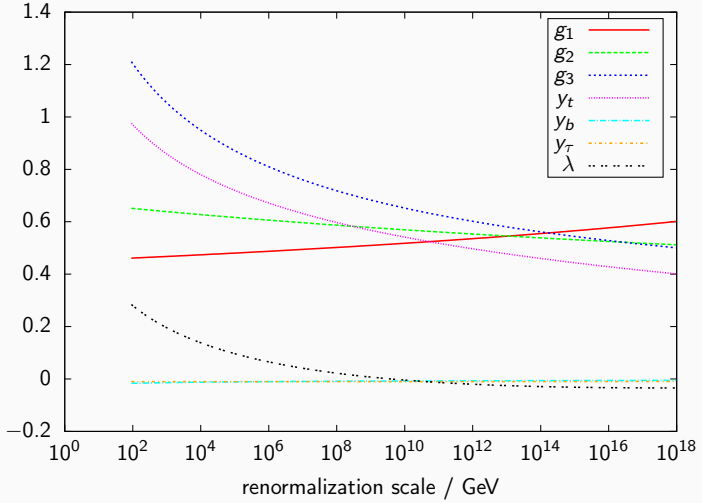

Di-Higgs pheomonology

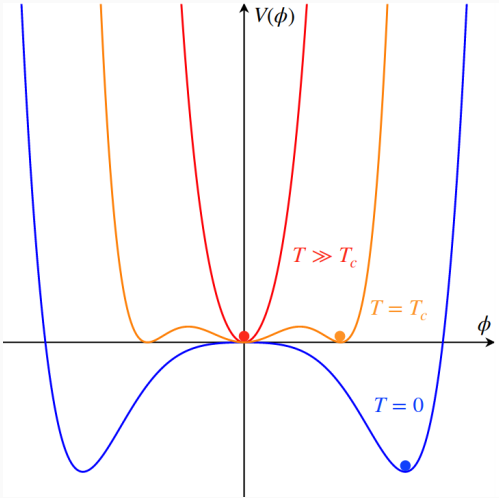

first order

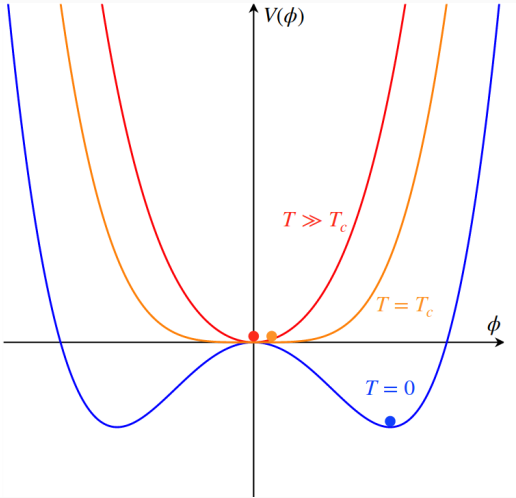

second order

Di-Higgs cross-section

$$A(\lambda_t, \lambda_{HHH}) \equiv \lambda_t^2 \cdot \square + \lambda_t \cdot \lambda_{HHH} \triangle$$

$$\sigma \approx k_t^4 \left[|\square|^2 + \frac{k_\lambda}{k_t}(\square \triangle + \triangle \square) + \left(\frac{k_\lambda}{k_t}\right)^2 |\triangle|^2 \right]$$

- minimum cross-section at $\kappa_\lambda = 2.4\kappa_t$
- minimum m_{HH} at $m_{HH} = 2m_t$ for $\kappa_\lambda = 2$
- $\sigma^{\text{NNLO}}_{\text{ggF HH}} = 31.05^{+2.2\%}_{-5.0\%}$ fb
- $\sigma^{\text{NNLO}}_{\text{VBF HH}} = 1.723^{+0.03\%}_{-0.04\%}$ fb

per t	1 H per 1s	3 HH per 1h	1 HH($b\bar{b}\gamma\gamma$) per 5d
per pp	2.5 10^{-9} H	2 10^{-11} HH	6.25 10^{-16} 2H

Di-Higgs production modes

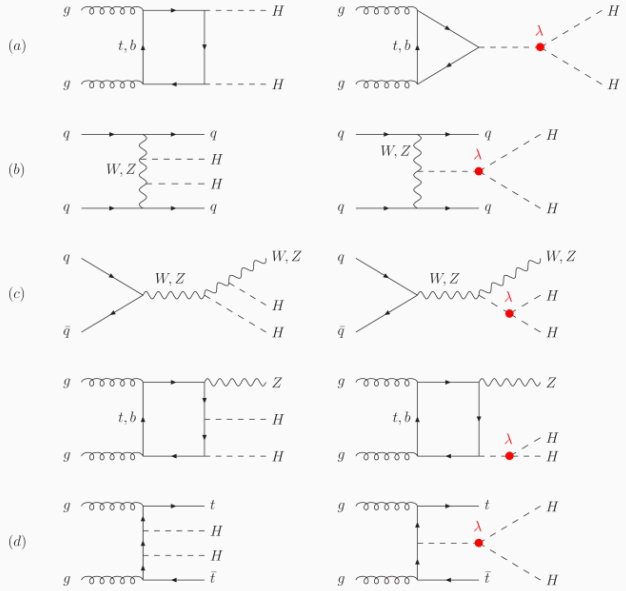

Di-Higgs cross-section as function of $\sqrt{s}$

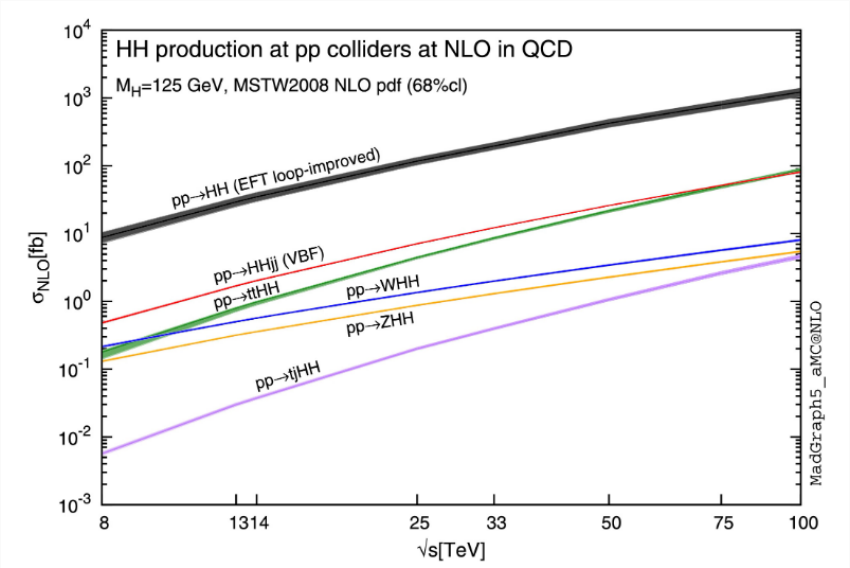

LHC accelerator chain

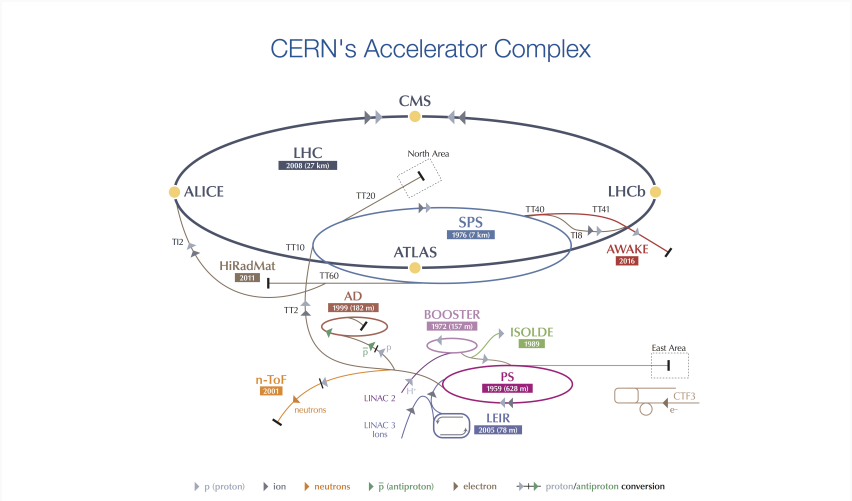

LHC planning

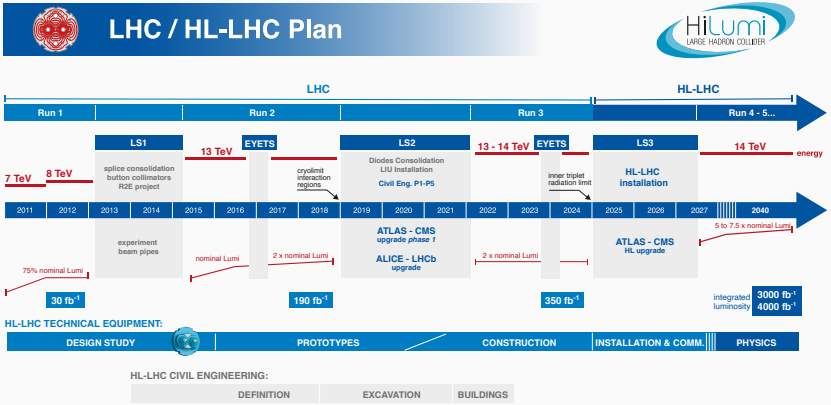

Pile-Up

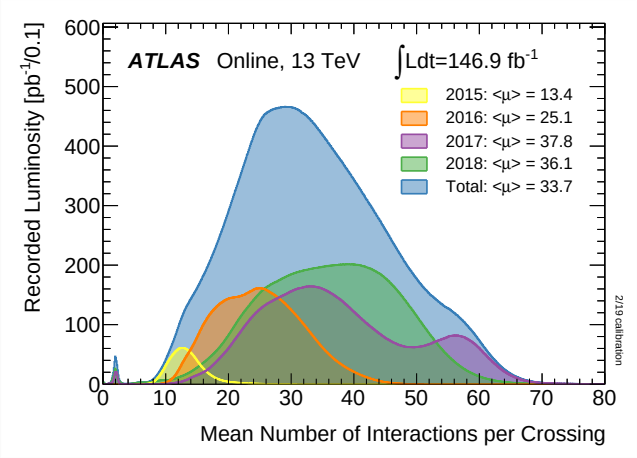
ATLAS Online, 13 TeV
∫Ldt=146.9 fb-1
2015: <μ> = 13.4
2016: <μ> = 25.1
2017: <μ> = 37.8
2018: <μ> = 36.1
Total: <μ> = 33.7
Recorded Luminosity [pb-1/0.1]
Mean Number of Interactions per Crossing
2/19 calibration

Object reconstruction

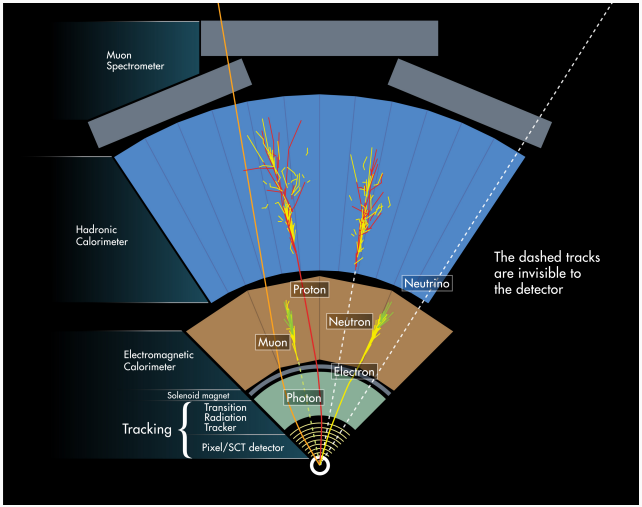

HH$\to b\bar{b}\gamma\gamma$ 36 fb^{-1}

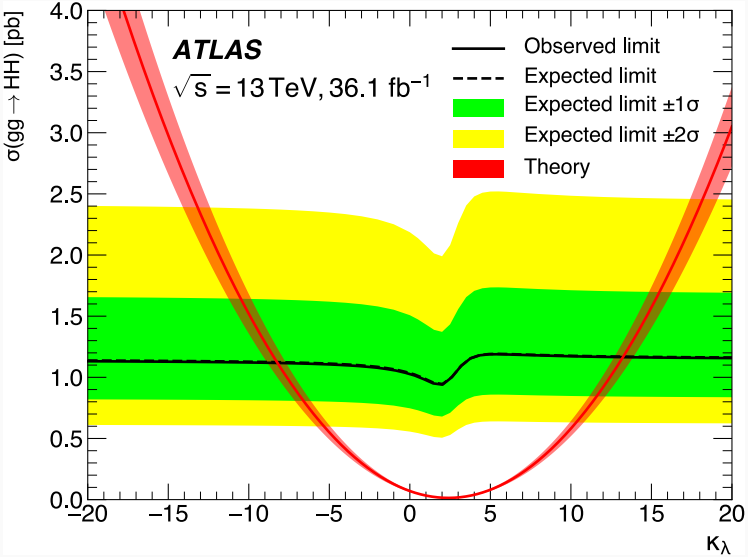

Simulation

Process	Generator	PDF set	Showering	Tune
ggF	NNLOPS	PDFLHC	Pythia 8.2	AZNLO
VBF	Powheg Box v2	PDFLHC	Pythia 8.2	AZNLO
WH	Powheg Box v2	PDFLHC	Pythia 8.2	AZNLO
$qq \to ZH$	Powheg Box v2	PDFLHC	Pythia 8.2	AZNLO
$gg \to ZH$	Powheg Box v2	PDFLHC	Pythia 8.2	AZNLO
$t\bar{t}H$	Powheg Box v2	NNPDF3.0nlo	Pythia 8.2	A14
bbH	Powheg Box v2	NNPDF3.0nlo	Pythia 8.2	A14
$tHqj$	MadGraph5_aMC@NLO	NNPDF3.0nlo	Pythia 8.2	A14
tHW	MadGraph5_aMC@NLO	NNPDF3.0nlo	Pythia 8.2	A14
$\gamma\gamma$+jets	Sherpa v2.2.4	NNPDF3.0nnlo	Sherpa v2.2.4	–
$t\bar{t}\gamma\gamma$	MadGraph5_aMC@NLO	NNPDF2.3lo	Pythia 8.2	–

Di-photon trigger efficiency

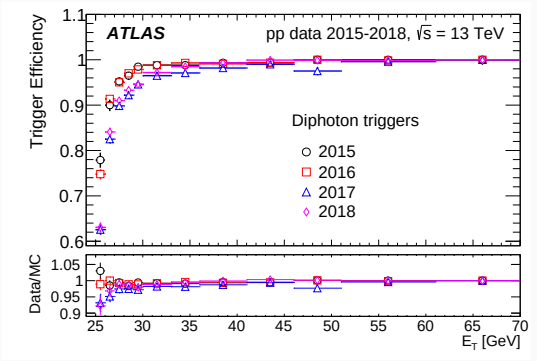

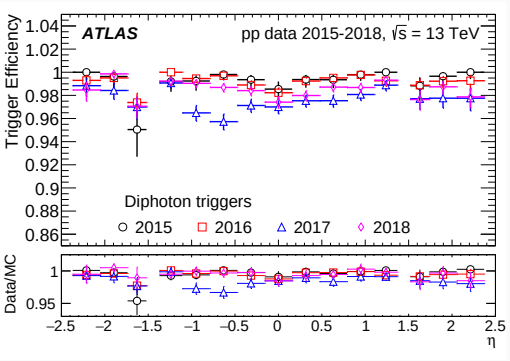

b-jet calibration chain

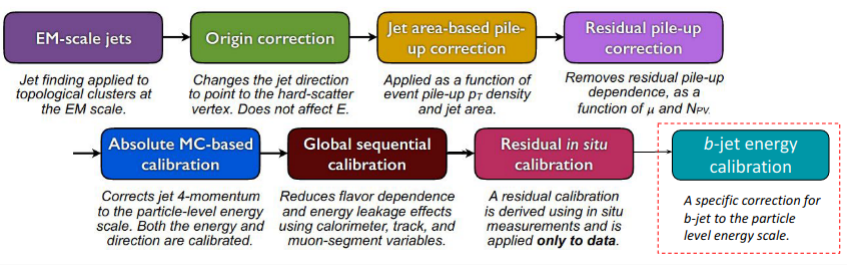

μ-in-jet correction selection

Criteria	Selection
p_T	> 4 GeV
ID	Medium
ΔR	$< \min(0.4, 0.004 + 10/p_T)$

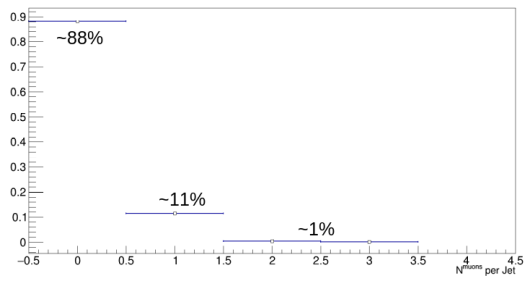

p_TReco correction

- Target $\rightarrow$ *TruthWZ* jets, contains reconstructed jets with all stable hadrons and non-isolated muons and neutrinos. $\Delta R(jet^{truth}, jet^{reco})$
- Correction = mean of the $\frac{p_T^{truth}}{p_T^{reco}}$ distribution

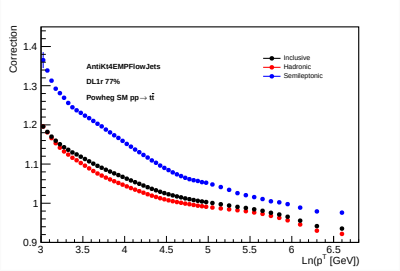

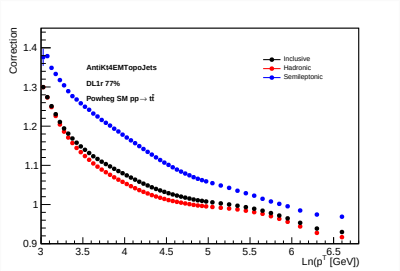

p_TReco gain

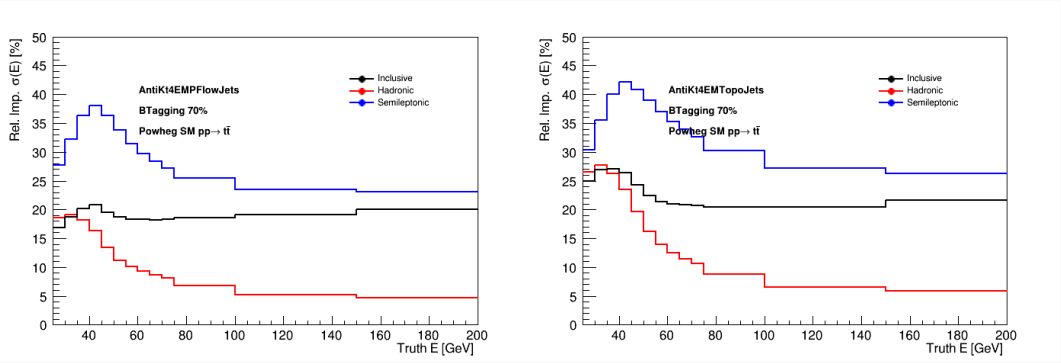
AntiKt4EMPFlowJets
BTagging 70%
Powheg SM pp→ tt̄
Inclusive
Hadronic
Semileptonic
Rel. Imp. σ(E) [%]
Truth E [GeV]
AntiKt4EMTopoJets
BTagging 70%
Powheg SM pp→ tt̄
Inclusive
Hadronic
Semileptonic
Rel. Imp. σ(E) [%]
Truth E [GeV]

m_{bb} correction in each step

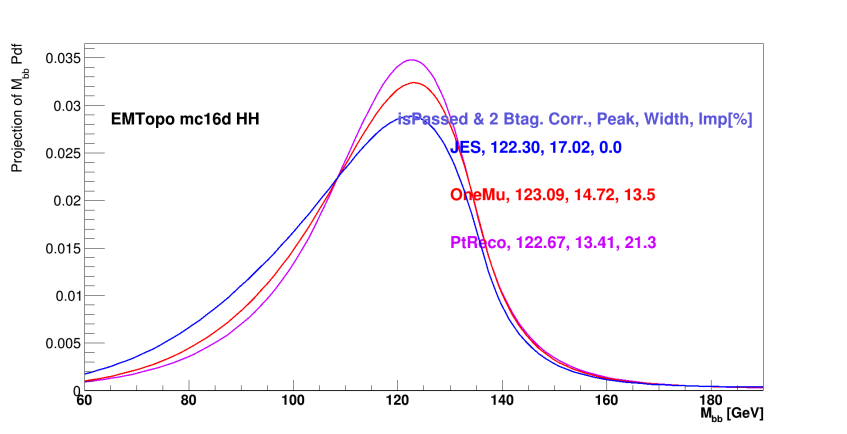

topological vs particle flow m_{bb}

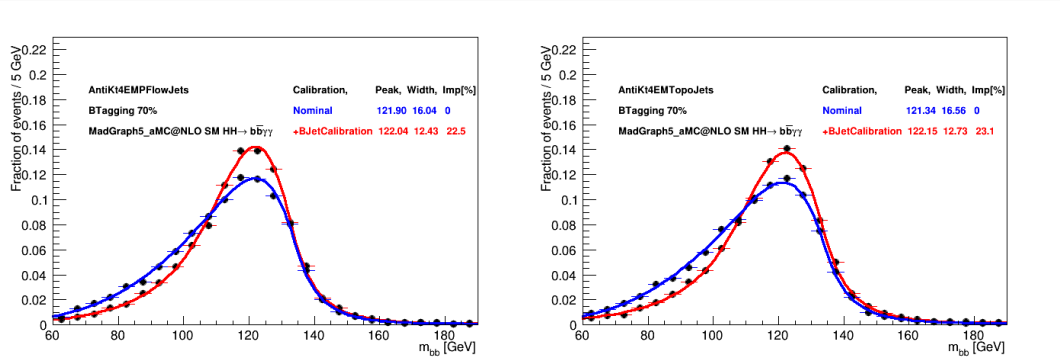

Impact on ZH background

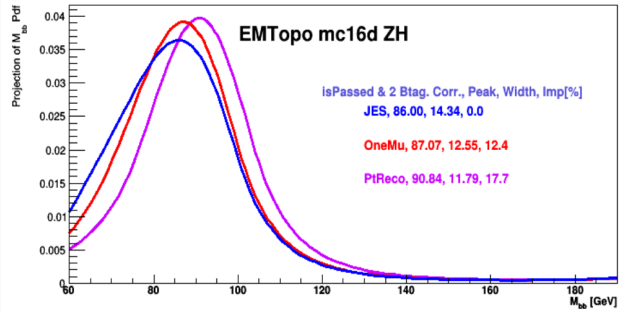

Impact on $t\bar{t}$H background

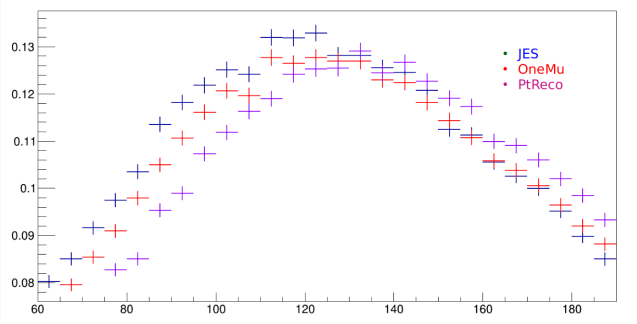

Neural Network vs μ-in-jet+p_TReco

- μ-in-jet+p_TReco compared to simple NN version.
- NN trained on $t\bar{t}$ sample
- Comparison performed on HH$\rightarrow b\bar{b}b\bar{b}$

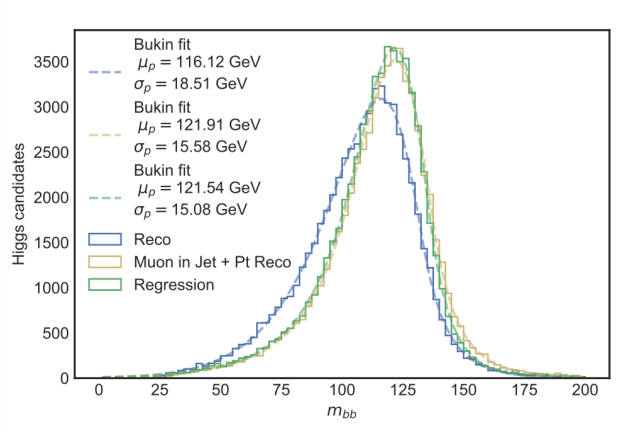

Motivation for $m^*_{b\bar{b}\gamma\gamma}$

- Improve resolution mainly for resonance analysis

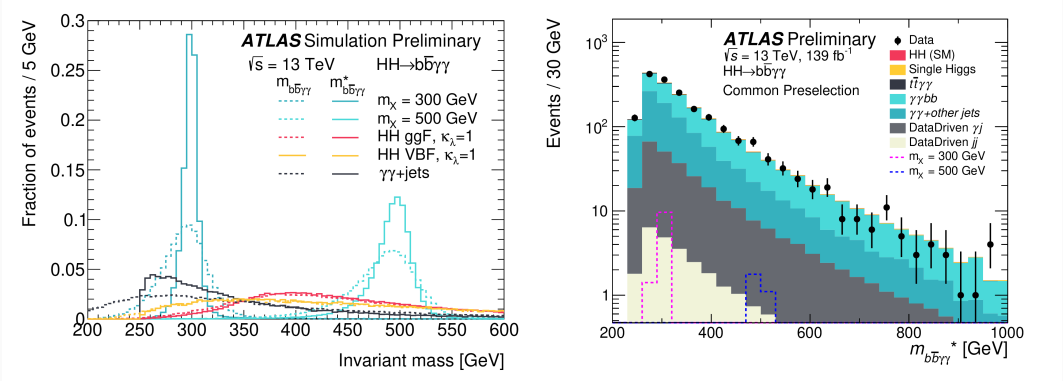

$m^*_{b\bar{b}\gamma\gamma}$ distribution

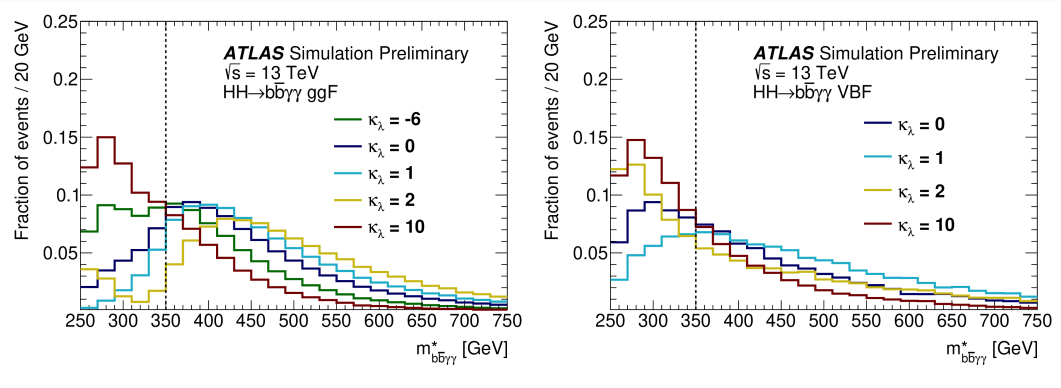

MVA inputs

Variable	Definition
Photon-related kinematic variables	
$p_T/m_{\gamma\gamma}$	Transverse momentum of the two photons scaled by their invariant mass $m_{\gamma\gamma}$
η and ϕ	Pseudo-rapidity and azimuthal angle of the leading and sub-leading photon
Jet-related kinematic variables	
b-tag status	Highest fixed b-tag working point that the jet passes
p_T, η and ϕ	Transverse momentum, pseudo-rapidity and azimuthal angle of the two jets with the highest b-tagging score
$p_T^{b\bar{b}}$, $\eta_{b\bar{b}}$ and $\phi_{b\bar{b}}$	Transverse momentum, pseudo-rapidity and azimuthal angle of b-tagged jets system
$m_{b\bar{b}}$	Invariant mass built with the two jets with the highest b-tagging score
H_T	Scalar sum of the p_T of the jets in the event
Single topness	For the definition, see Eq. (**??**)
Missing transverse momentum-related variables	
E_T^{miss} and ϕ^{miss}	Missing transverse momentum and its azimuthal angle

$$\chi_{Wt} = \min \sqrt{\left(\frac{m_{j_1 j_2} - m_W}{m_W}\right)^2 + \left(\frac{m_{j_1 j_2 j_3} - m_t}{m_t}\right)^2}$$

Variables distributions

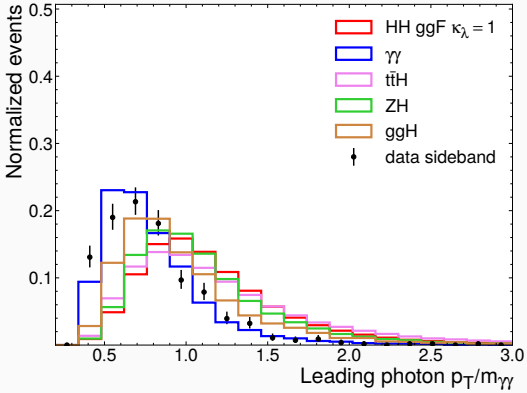

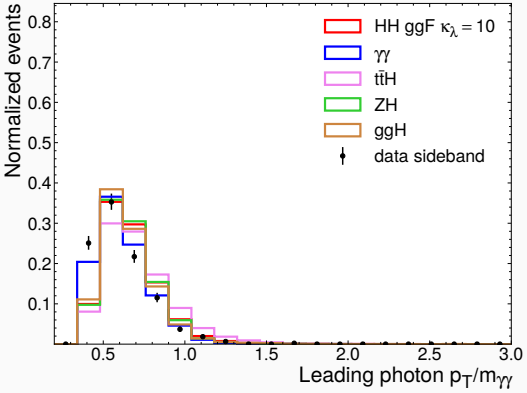

Variables distributions

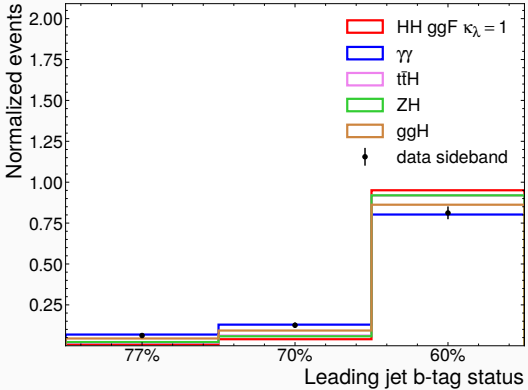

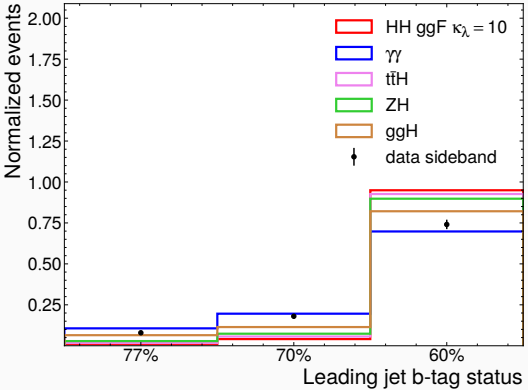

Variables distributions

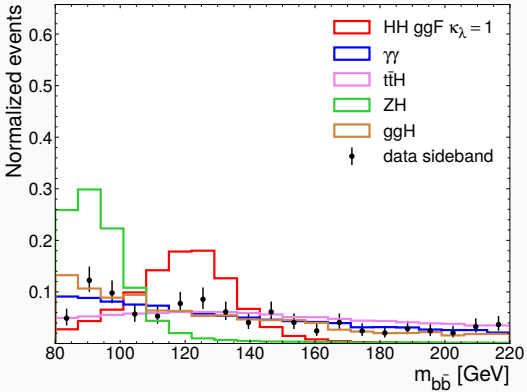

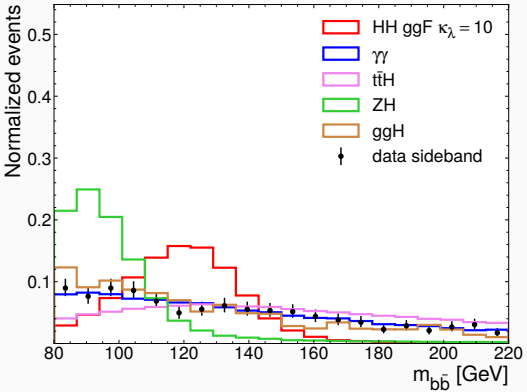

Variables distributions

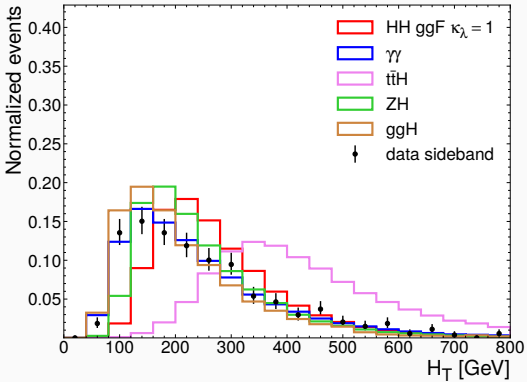

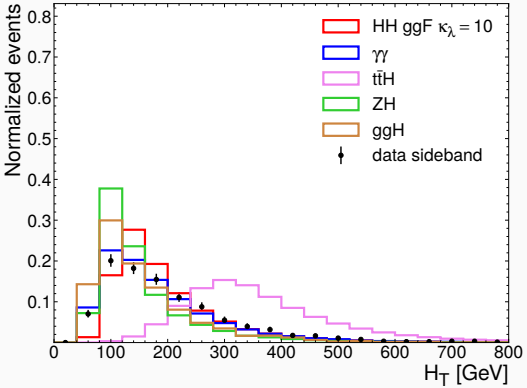

Variables distributions

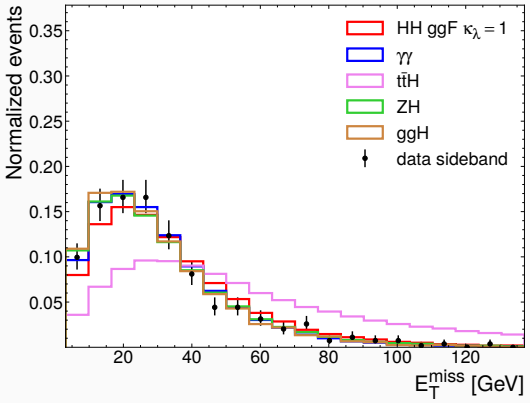

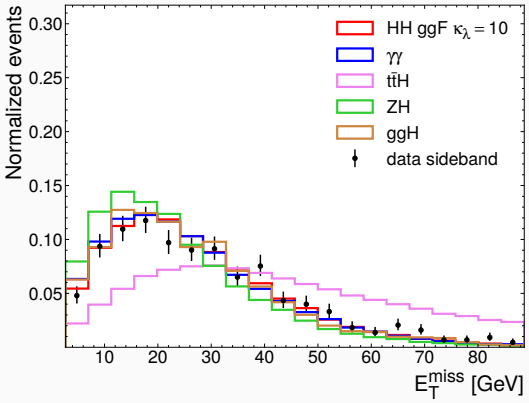

Variables distributions

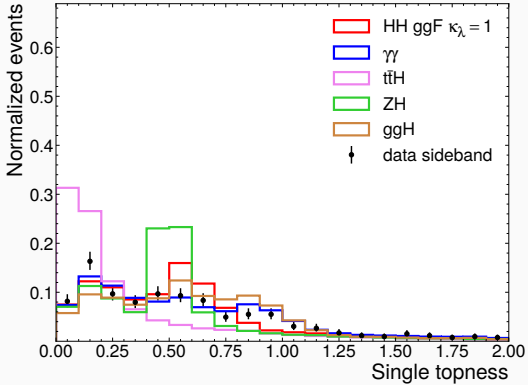

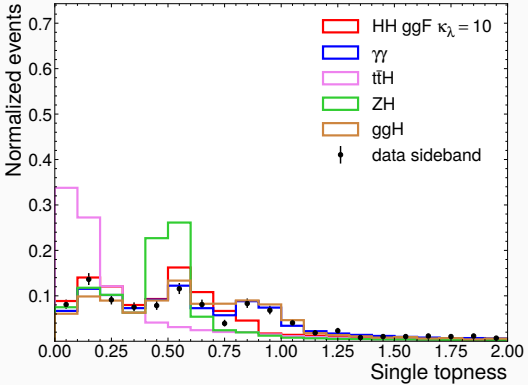

DNN loss function

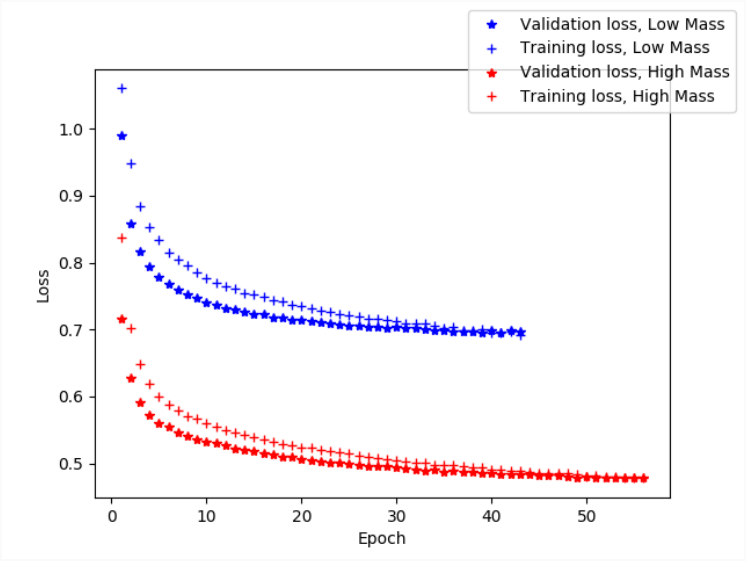

DNN confusion matrix

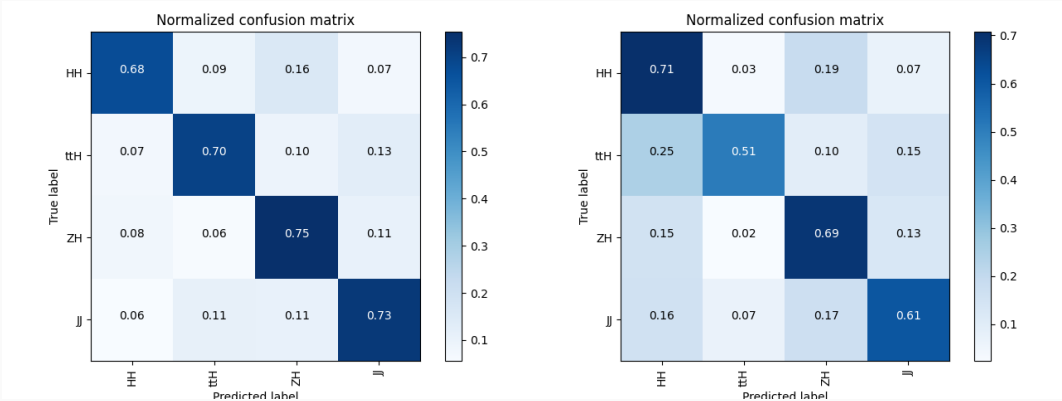

JJ = continuum $\gamma\gamma$+jets

d_{HH} distribution

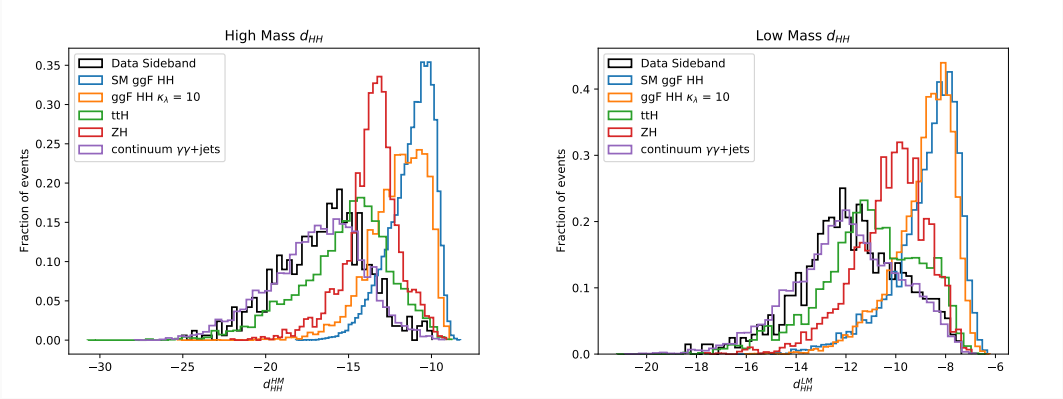

DNN significance breakdwon

Categories	SM ggF HH	BSM κ_λ=10 ggF HH
High mass, High d_{HH}	0.53	2.45
High mass, Low d_{HH}	0.11	0.94
Low mass, High d_{HH}	0.03	2.21
Low mass, Low d_{HH}	0.01	0.54
Combined	0.54σ	3.47σ

BDT categories

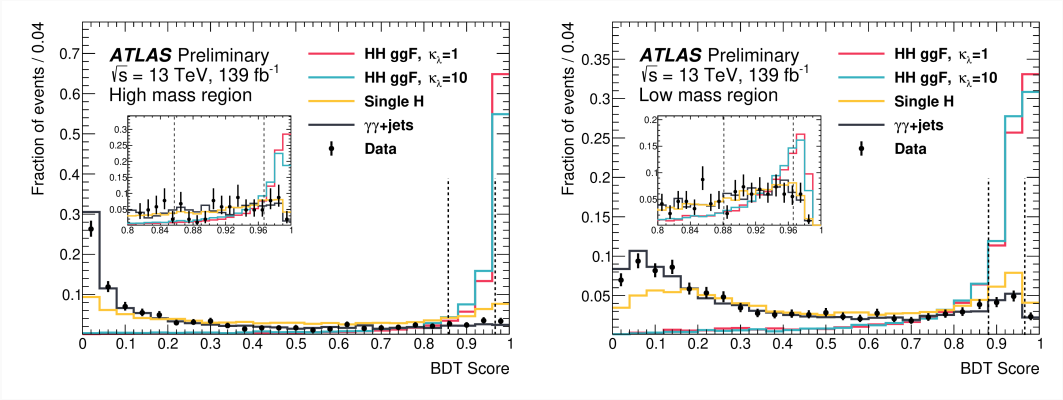

Category	Selection criteria
High mass BDT tight	$m^*_{bb\gamma\gamma} \geq 350$ GeV, BDT score $\in [0.967, 1]$
High mass BDT loose	$m^*_{bb\gamma\gamma} \geq 350$ GeV, BDT score $\in [0.857, 0.967]$
Low mass BDT tight	$m^*_{bb\gamma\gamma} < 350$ GeV, BDT score $\in [0.966, 1]$
Low mass BDT loose	$m^*_{bb\gamma\gamma} < 350$ GeV, BDT score $\in [0.881, 0.966]$

Analysis categories

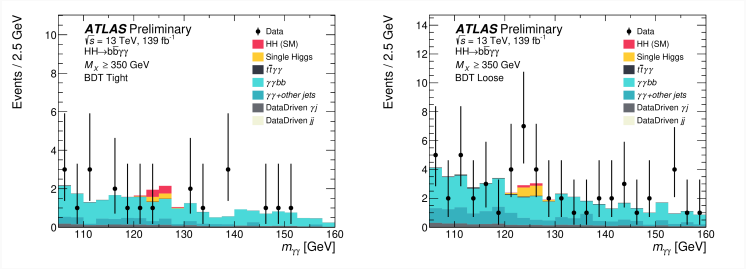

Statistical model

$$\mathcal{L} = \prod_c \left(Pois\left(n_c \mid N_c(\theta)\right) \cdot \prod_{i=1}^{n_c} f_c\left(m^i_{\gamma\gamma}, \theta\right) \cdot G(\theta) \right),$$

$$N_c(\theta) = \mu \cdot N_{\mathrm{HH,c}}\left(\theta_{yield}\right) + N_{\mathrm{H,c}}\left(\theta_{yield}\right) + N_{\mathrm{SS,c}} \cdot \theta_{\mathrm{SS,c}} + N_{\mathsf{continuum,c}},$$

$$\tilde{q}_\mu = \begin{cases} -2\log \frac{L(\mu, \hat{\hat{\theta}}(\mu))}{L(0, \hat{\hat{\theta}}(0))} & \hat{\mu} < 0 \\ -2\log \frac{L(\mu, \hat{\hat{\theta}}(\mu))}{L(\hat{\mu}, \hat{\theta})} & 0 \leq \hat{\mu} \leq \mu \\ 0 & \hat{\mu} > \mu \end{cases}$$

Modelling and Spurious Signal

- Biases related to the choice quantified through the Spurious Signal (SS) method:
  - Measure residual fitted N_{SS} in continuum MC: $n_{sig} \times PDF_{sig} + n_{bkg} \times PDF_{bkg}$
  - $N_{SS} = \max|n_{sig}(m_H)|$: m_H vary from 121 to 129 with step of 1 GeV
  - Relaxed SS criteria (allowing 2σ local statistical fluctuation) is used because of lack of statistics.

$$\zeta_{\mathrm{SS}} = \begin{cases} N_{\mathrm{SS}} + 2\Delta_{\mathrm{MC}}, & N_{\mathrm{SS}} + 2\Delta_{\mathrm{MC}} < 0 \\ N_{\mathrm{SS}} - 2\Delta_{\mathrm{MC}}, & N_{\mathrm{SS}} - 2\Delta_{\mathrm{MC}} > 0 \\ 0, & \textit{otherwise} \end{cases}$$

- Functional form chosen: **Exponential**
- The fitted N_{SS} are used as systematic uncertainties on the signal yield

Category	N_{SS}
High mass BDT tight	0.688
High mass BDT loose	0.990
Low mass BDT tight	0.594
Low mass BDT loose	1.088

b-jet energy calibration systematic

- μ-in-jet systematic negligible from Run-1 in ZH
- Impact of b-tagging WP on p_TReco, as systematic
  - three variations of the p_TReco correction, using 60%, 70% and 85% b-tagging WP.
  - relative impact on the yield $\rightarrow$ systematic uncertainty
  - largest systematic, same order as the flavour tagging uncertainty

p_T-Reco variation	% relative effect to nominal
60% WP	$\pm$ 0.094
70% WP	$\pm$ 0.065
85% WP	$\pm$ 0.12

p_TReco as function of b-tagging WPs

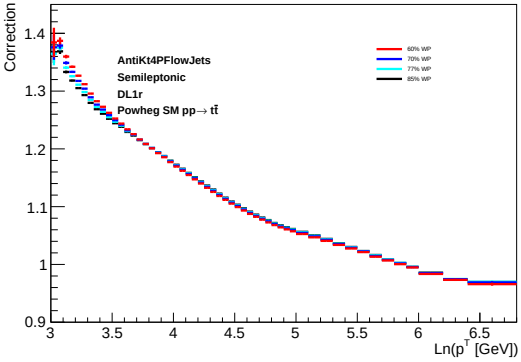

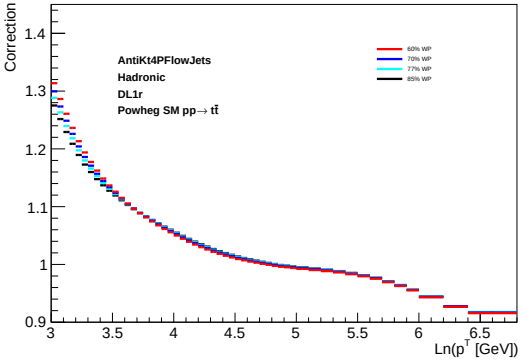

background-only fit

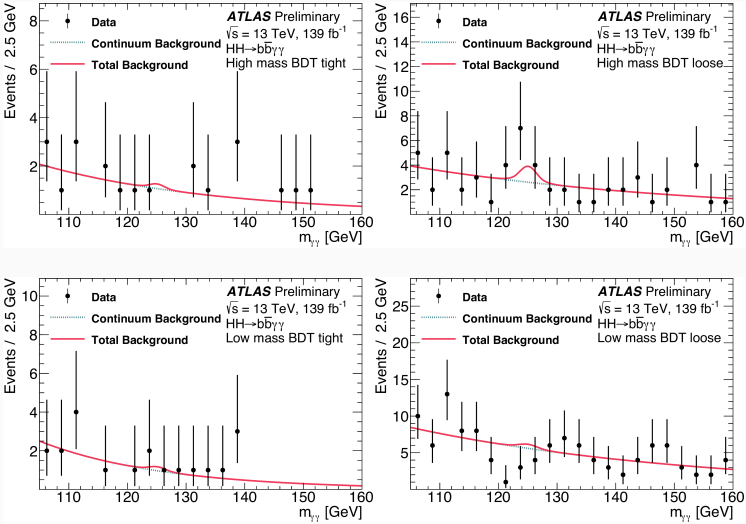

Observed events

	High mass BDT tight	High mass BDT loose	Low mass BDT tight	Low mass BDT loose
Continuum background	4.9 ± 1.1	9.5 ± 1.5	3.7 ± 1.0	24.9 ± 2.5
Single Higgs boson background	0.670 ± 0.032	1.57 ± 0.04	0.220 ± 0.016	1.39 ± 0.04
ggF	0.261 ± 0.028	0.44 ± 0.04	0.063 ± 0.014	0.274 ± 0.030
$t\bar{t}H$	0.1929 ± 0.0045	0.491 ± 0.007	0.1074 ± 0.0033	0.742 ± 0.009
ZH	0.142 ± 0.005	0.486 ± 0.010	0.04019 ± 0.0027	0.269 ± 0.007
Rest	0.074 ± 0.012	0.155 ± 0.020	0.008 ± 0.006	0.109 ± 0.016
SM HH signal	0.8753 ± 0.0032	0.3680 ± 0.0020	$(49.4 \pm 0.7) \cdot 10^{-3}$	$(78.7 \pm 0.9) \cdot 10^{-3}$
ggF	0.8626 ± 0.0032	0.3518 ± 0.0020	$(46.1 \pm 0.7) \cdot 10^{-3}$	$(71.8 \pm 0.9) \cdot 10^{-3}$
VBF	0.01266 ± 0.00016	0.01618 ± 0.00018	$(3.22 \pm 0.08) \cdot 10^{-3}$	$(6.923 \pm 0.011) \cdot 10^{-3}$
Alternative $HH(\kappa_\lambda = 10)$ signal	6.36 ± 0.05	3.691 ± 0.038	4.65 ± 0.04	8.64 ± 0.06
Data	2	17	5	14

Systematic impact

		Relative impact of the systematic uncertainties in %	
Source	Type	Non-resonant analysis HH	Resonant analysis m_X = 300 GeV
Experimental			
Photon energy scale	Norm. + Shape	5.2	2.7
Photon energy resolution	Norm. + Shape	1.8	1.6
Flavor tagging	Normalization	0.5	< 0.5
Theoretical			
Heavy flavor content	Normalization	1.5	< 0.5
Higgs boson mass	Norm. + Shape	1.8	< 0.5
PDF+α_s	Normalization	0.7	< 0.5
Spurious signal	Normalization	5.5	5.4

Expected limit: Stat. Only vs Stat.+Syst.

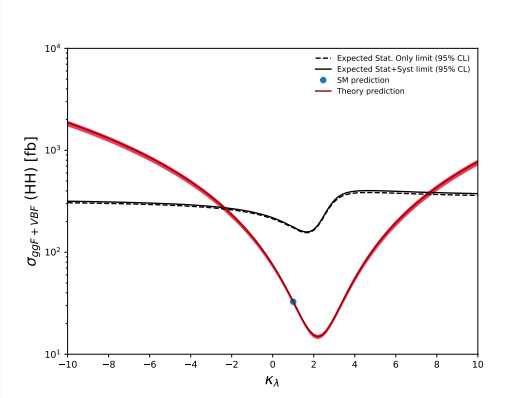

	Stat. Only	Stat.+Syst.
$\sigma_{HH}/\sigma_{HH}^{SM}$ limit	5.3	5.5
κ_λ interval	[-2.3, 7.6]	[-2.4, 7.7]

Category	$\sigma_{HH}/\sigma_{HH}^{SM}$ limit
High mass, High BDT	5.8
High mass, Low BDT	21.0
Low mass, High BDT	102.9
Low mass, Low BDT	125.6
Combined	5.5

κ_λ likelihood scan

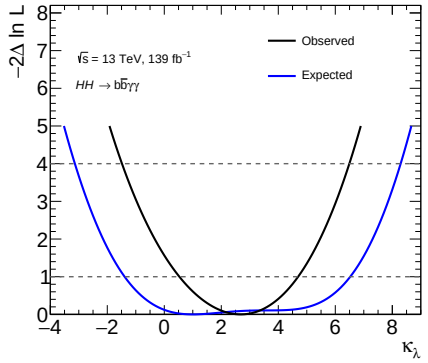

- best-fit κ_λ is $2.7^{+2.1}_{-2.2}$
- $\mu_{HH} = 1 \pm 2.37$ for SM

	1σ CI	2σ CI
Expected	[-1.4, 6.4]	[-3.1, 8.2]
Observed	[0.5, 4.7]	[-1.4, 6.5]

Combination with CMS

- ATLAS+CMS $\sim \times 2$ 139 fb^{-1}
- Expected 95% CL limit on σ_{HH} of 3.4

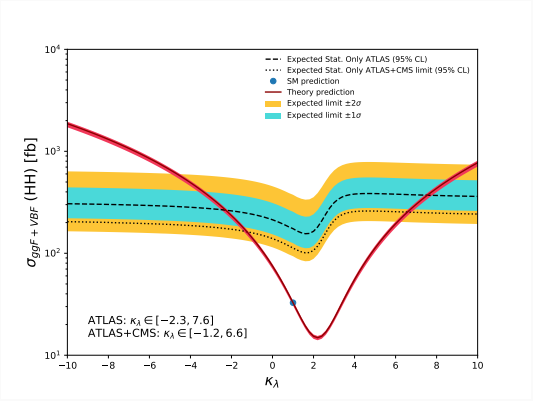

full Run-2 $HH \to b\bar{b}\tau^+\tau^-$

ATLAS-CONF-2021-030

- Relies on:
  - $\tau_{had}\tau_{had}$: Single and Double tau trigger
  - $\tau_{lep}\tau_{had}$: Single lepton an lepton+tau trigger
- backgrounds:
  - **true** τ: $t\bar{t}$ and Z+HF, from Monte Carlo and normalization from data
  - **fake** τ: $t\bar{t}$ and multi-jet, data driven
- 3 MVA categories:
  - $\tau_{had}\tau_{had}$
  - $\tau_{lep}\tau_{had}$
  - Z+HF background control
- fit of MVA outputs

		Observed	$-2\,\sigma$	$-1\,\sigma$	Expected	$+1\,\sigma$	$+2\,\sigma$
$\tau_{\text{had}}\tau_{\text{had}}$	$\sigma_{\text{ggF+VBF}}$ [fb]	145	70.5	94.6	131	183	245
	$\sigma_{\text{ggF+VBF}}/\sigma^{\text{SM}}_{\text{ggF+VBF}}$	4.95	2.38	3.19	4.43	6.17	8.27
$\tau_{\text{lep}}\tau_{\text{had}}$	$\sigma_{\text{ggF+VBF}}$ [fb]	265	124	167	231	322	432
	$\sigma_{\text{ggF+VBF}}/\sigma^{\text{SM}}_{\text{ggF+VBF}}$	9.16	4.22	5.66	7.86	10.9	14.7
Combined	$\sigma_{\text{ggF+VBF}}$ [fb]	135	61.3	82.3	114	159	213
	$\sigma_{\text{ggF+VBF}}/\sigma^{\text{SM}}_{\text{ggF+VBF}}$	4.65	2.08	2.79	3.87	5.39	7.22

- $\times 4$ improvement w.r.t early Run-2 ($12.7\times$SM)
- large systematic from background modelling

full Run-2 HH$\rightarrow b\bar{b}\tau^+\tau^-$

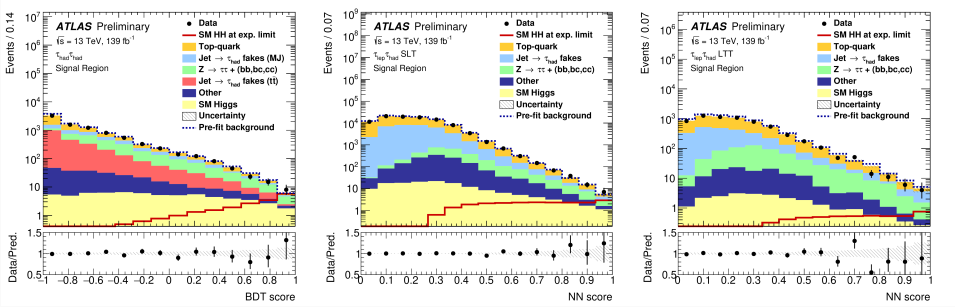

Early Run-2 combination

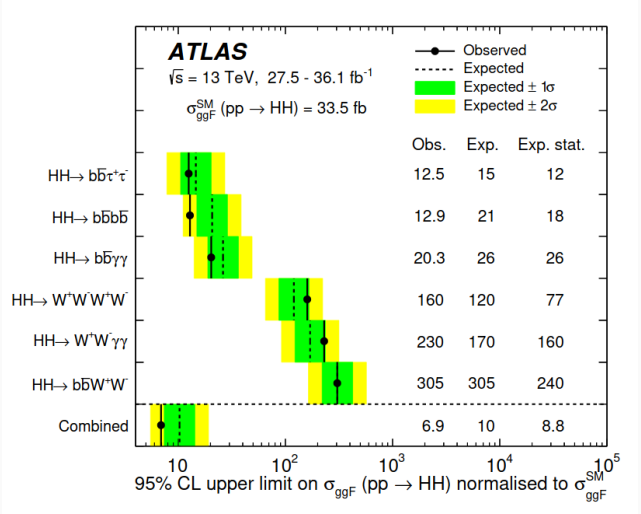

First full Run-2 combination

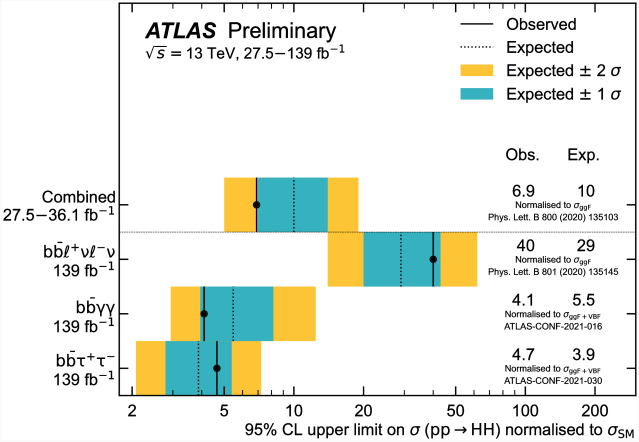

Single Higgs vs κ_λ

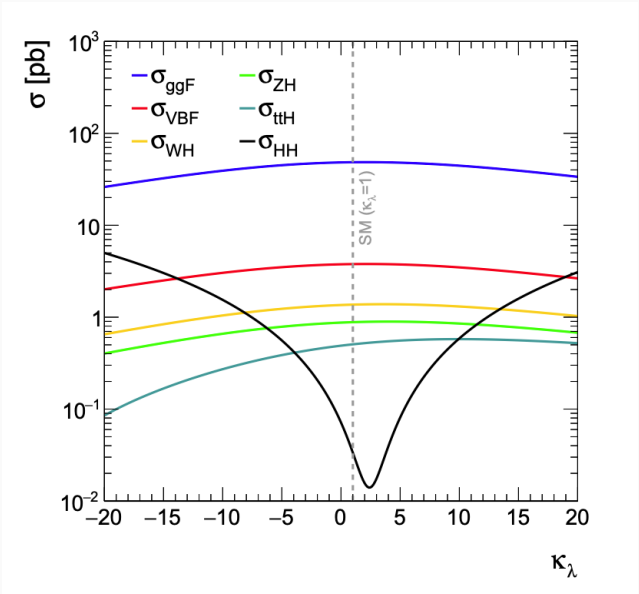

H+HH

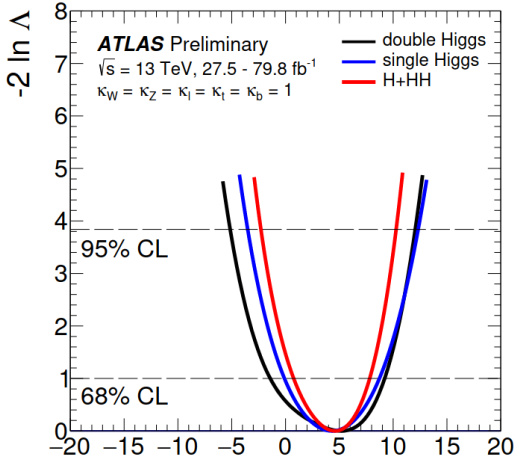

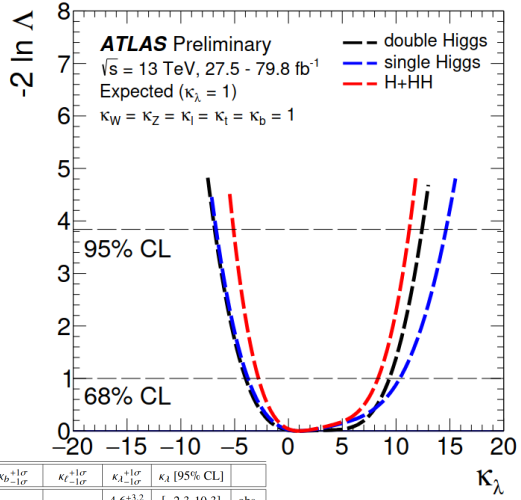

Model	$\kappa_W^{+1\sigma}_{-1\sigma}$	$\kappa_Z^{+1\sigma}_{-1\sigma}$	$\kappa_t^{+1\sigma}_{-1\sigma}$	$\kappa_b^{+1\sigma}_{-1\sigma}$	$\kappa_\ell^{+1\sigma}_{-1\sigma}$	$\kappa_\lambda^{+1\sigma}_{-1\sigma}$	κ_λ [95% CL]	
κ_λ-only	1	1	1	1	1	$4.6^{+3.2}_{-3.8}$	[−2.3, 10.3]	obs.
						$1.0^{+7.3}_{-3.8}$	[−5.1, 11.2]	exp.
Generic	$1.03^{+0.08}_{-0.08}$	$1.10^{+0.09}_{-0.09}$	$1.00^{+0.12}_{-0.11}$	$1.03^{+0.20}_{-0.18}$	$1.06^{+0.16}_{-0.16}$	$5.5^{+3.5}_{-5.2}$	[−3.7, 11.5]	obs.
	$1.00^{+0.08}_{-0.08}$	$1.00^{+0.08}_{-0.08}$	$1.00^{+0.12}_{-0.12}$	$1.00^{+0.21}_{-0.19}$	$1.00^{+0.16}_{-0.15}$	$1.0^{+7.6}_{-4.5}$	[−6.2, 11.6]	exp.

Cross-section as function of c_i

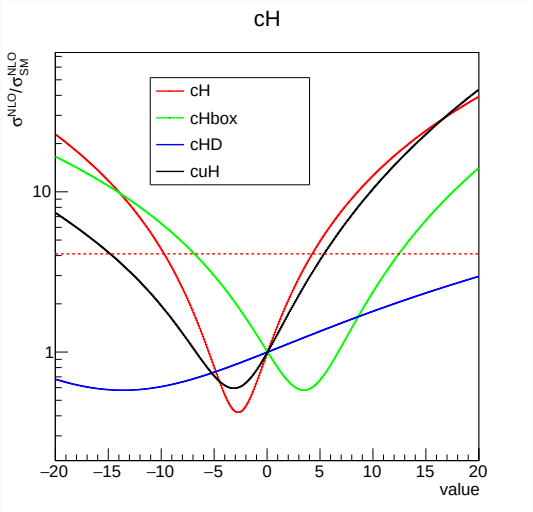

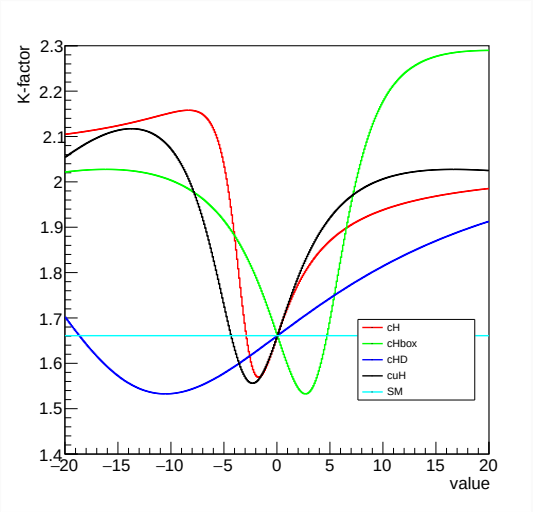

Linear vs quadratic : m_{HH} distribution

Interference

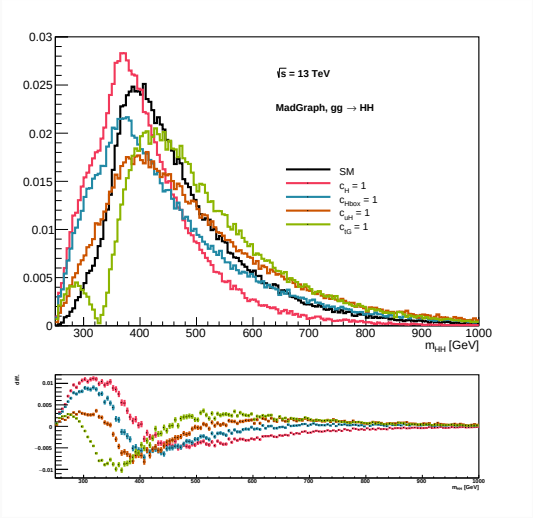

pure BSM

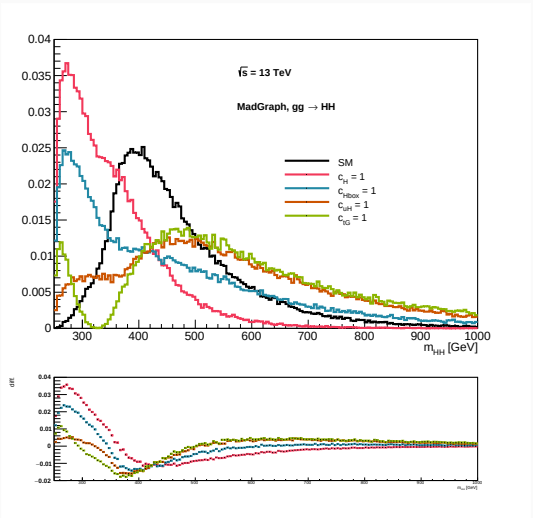

Linear vs quadratic : Cross-section

Interference

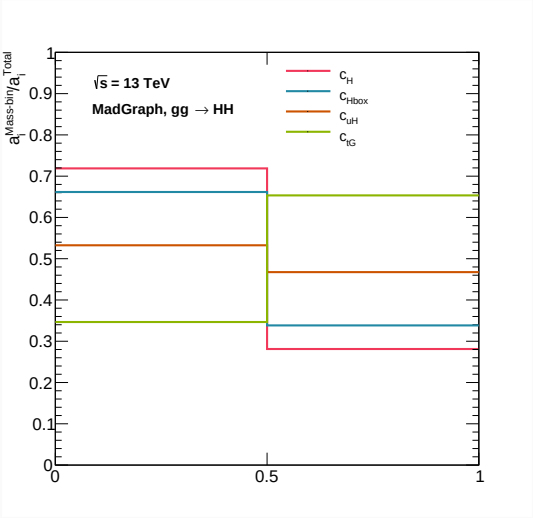

pure BSM

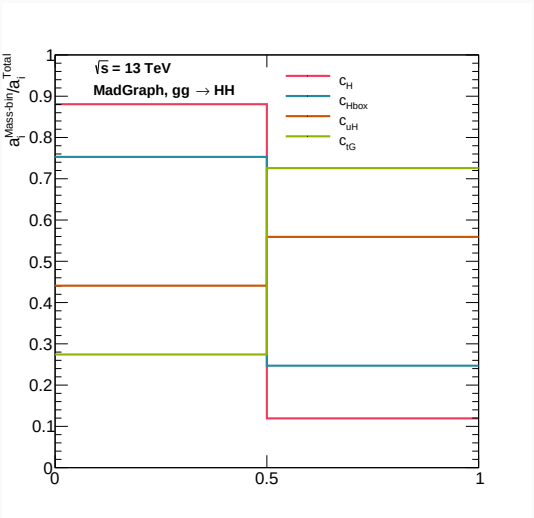

Cross-section parameterization

- ggF HH events simulated using MadGraph events generator + SMEFTatNLO feynrules model (using NLO card).
- Each term (linear and quadratic) is generated separately:

Command	term
generate p p > h h QED=2 QCD=2 NP=2 [QCD]	SM only
generate p p > h h NP=2 QCD=2 QED=2 NP^2==2 [QCD]	Interference
generate p p > h h NP=2 QCD=2 QED=2 NP^2==4 [QCD]	BSM only

- 4 EFT variations are generated for each operator, $c_i = \pm 1, \pm 2$
- $\frac{\sigma}{\sigma_{SM}}$ fitted in each mass region (High mass and Low mass) using
- Cross-term effect considered by generating an additional $c_{i,j} = 1$ BSM sample and subtract individual quadratic contribution.

c_H parameterization

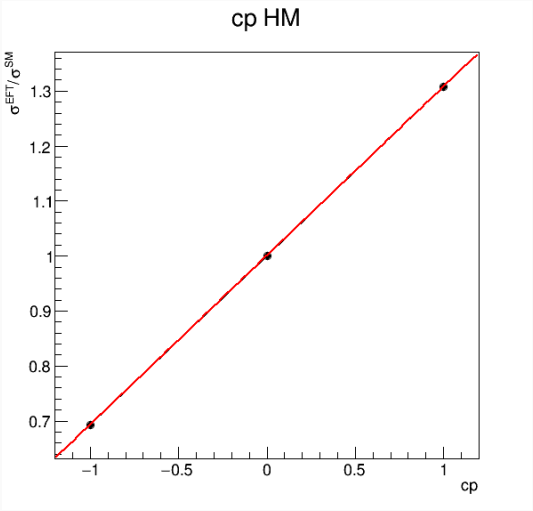

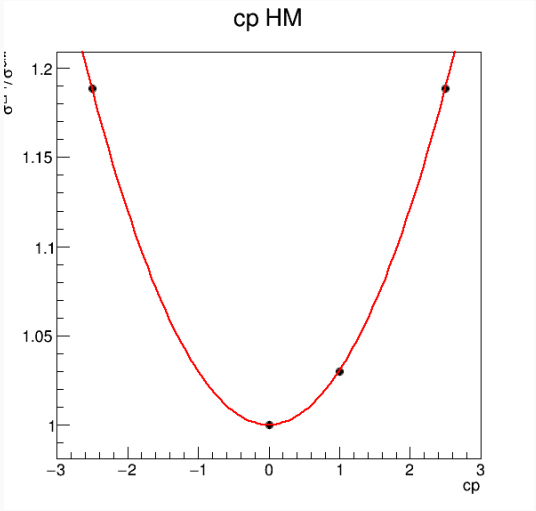

Parametrization

Region	σ/σ_{SM}
High mass	$- 0.19 \cdot c_{H\Box} + 0.02 \cdot c_{H\Box}^2 + 0.31 \cdot c_H$ $+ 0.03 \cdot c_H^2 + 0.24 \cdot c_{uH} + 0.03 \cdot c_{uH}^2$ $- 0.30 \cdot c_{tG} + 0.05 \cdot c_{tG}^2 - 0.04 \cdot c_H \cdot c_{H\Box}$ $+ 0.04 \cdot c_H \cdot c_{uH} - 0.06 \cdot c_H \cdot c_{tG}$ $- 0.05 \cdot c_{H\Box} \cdot c_{uH} + 0.04 \cdot c_{H\Box} \cdot c_{tG}$ $- 0.06 \cdot c_{uH} \cdot c_{tG}$
Low mass	$- 0.38 \cdot c_{H\Box} + 0.05 \cdot c_{H\Box}^2 + 0.79 \cdot c_H$ $+ 0.22 \cdot c_H^2 + 0.28 \cdot c_{uH} + 0.02 \cdot c_{uH}^2$ $- 0.16 \cdot c_{tG} + 0.02 \cdot c_{tG}^2 - 0.21 \cdot c_H \cdot c_{H\Box}$ $+ 0.14 \cdot c_H \cdot c_{uH} + 0.09 \cdot c_H \cdot c_{tG}$ $- 0.07 \cdot c_{H\Box} \cdot c_{uH} - 0.03 \cdot c_{H\Box} \cdot c_{tG}$ $+ 0.03 \cdot c_{uH} \cdot c_{tG}$

likelihood scans

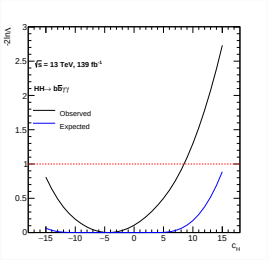

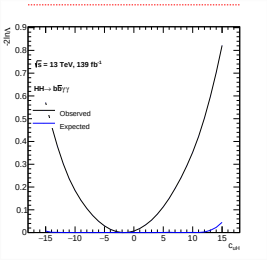

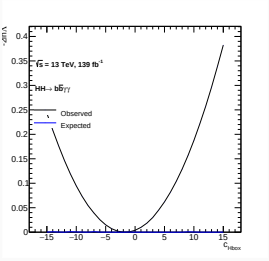

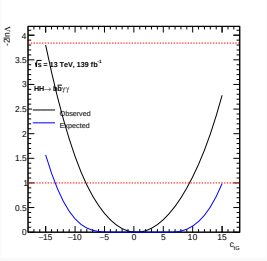

Sensitivity estimate

- Looking at the eigenvectors of the inverse covariance matrix of Wilson coefficients

$$C_{EFT}^{-1} = P^T \cdot C_{b\bar{b}\gamma\gamma}^{-1} \cdot P$$

- P is the parameterization matrix considering only linear terms.

Eigenvalue	Eigenvector
0.0523	- 0.582 $\cdot$ c_H + 0.363 $\cdot$ $c_{H\Box}$ - 0.456 $\cdot$ c_{uH} + 0.567 $\cdot$ c_{tG}
0.0001	- 0.696 $\cdot$ c_H + 0.182 $\cdot$ $c_{H\Box}$ + 0.206 $\cdot$ c_{uH} - 0.663 $\cdot$ c_{tG}
-0.0000	- 1.025 $\cdot$ c_H - 1.947 $\cdot$ $c_{H\Box}$ + 0.702 $\cdot$ c_{uH} + 0.759 $\cdot$ c_{tG}
-0.0000	- 0.235 $\cdot$ c_H - 0.006 $\cdot$ $c_{H\Box}$ + 0.977 $\cdot$ c_{uH} + 0.549 $\cdot$ c_{tG}

c_H only

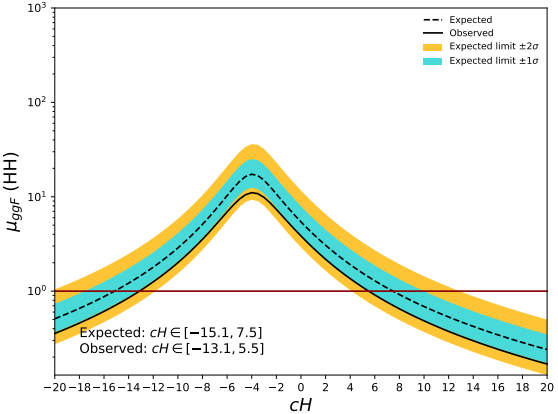
Expected
Observed
Expected limit ±2σ
Expected limit ±1σ
μ_{ggF} (HH)
10^3
10^2
10^1
10^0
Expected: $cH \in [-15.1, 7.5]$
Observed: $cH \in [-13.1, 5.5]$
−20 −18 −16 −14 −12 −10 −8 −6 −4 −2 0 2 4 6 8 10 12 14 16 18 20
cH

c_H vs κ_λ

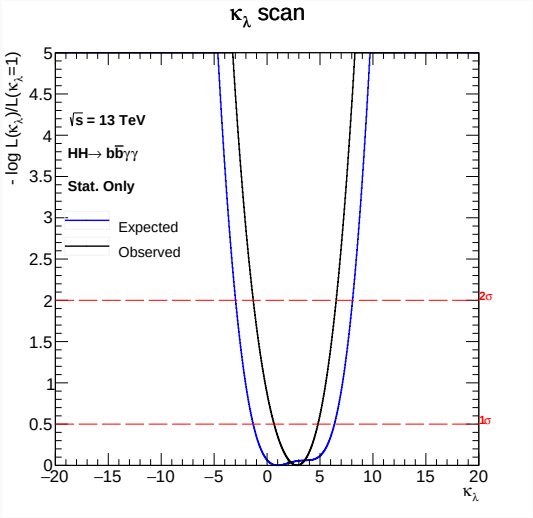

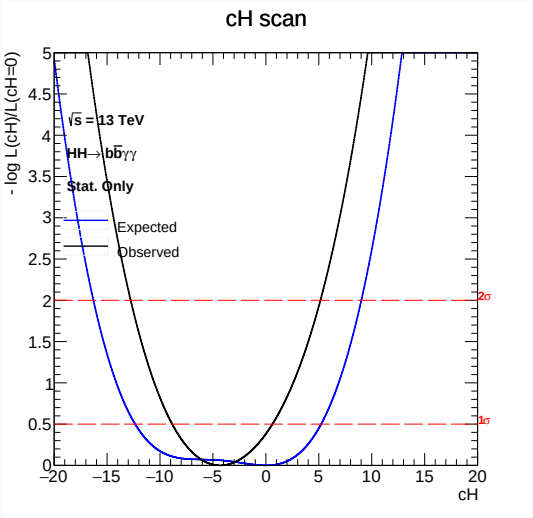

Linear vs Quadratic

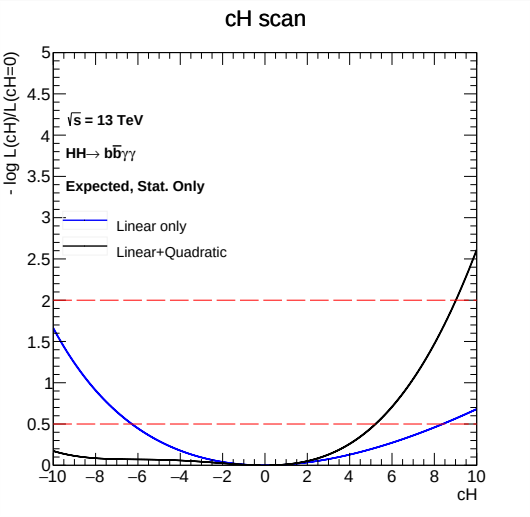

Extrapolation to Run-3

- Scale Run-2 with $300/139 \sim 2.16$
- Expected 95% CL limit on σ_{HH} of 3.3
- $\mu_{HH} = 1 \pm 1.52$ for SM
- SM HH significance: 0.71σ

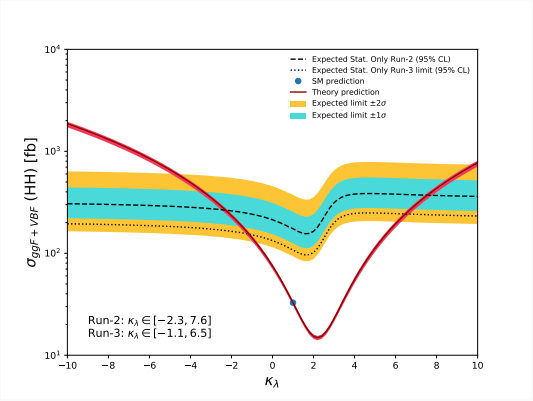

European strategy

- Monte Carlo based $b\bar{b}\gamma\gamma$ analysis
- One BDT category, 40% efficiency and 99% of background rejection
- Signal extracted using $m_{b\bar{b}\gamma\gamma}$ variable.
- $\mu = 1 \pm 0.6$ with significance of 2.1σ

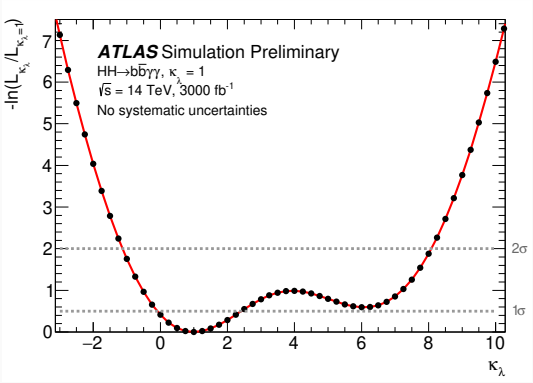

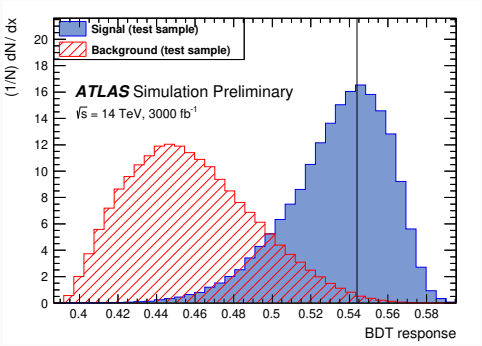

Scenario	1σ CI	2σ CI
Stat.	$-0.1 < \kappa_\lambda < 2.4$	$-1.1 < \kappa_\lambda < 8.1$
Syst.	$-0.2 < \kappa_\lambda < 2.5$	$-1.4 < \kappa_\lambda < 8.2$

Extrapolation to HL-LHC

Process	ggF HH	VBF HH	ggF H	VBF H	$t\bar{t}$H	WH	ZH	tHjb	tWH	$\gamma\gamma$
Scale	1.19	1.2	1.13	1.13	1.21	1.1	1.11	1.21	1.22	+18%

Scenario	Run-2 Stat. Only	HL-LHC Stat. Only
High mass, High BDT	0.47	2.38
High mass, Low BDT	0.13	0.64
Low mass, High BDT	0.03	0.15
Low mass, Low BDT	0.02	0.10
Combined	0.48σ	2.47σ

- $\mu_{HH} = 1 \pm 0.44$

Prospect in FCC-hh

2004.03505

- pp collider at $\sqrt{s} = 100$ TeV.
- $\mathcal{L}_{int} = 30$ ab^{-1}
- From 14 TeV to 100 TeV, $\times$ 30 increase in cross-section

	@68% CL	scenario I	scenario II	scenario III
δ_μ	stat only	2.5	3.6	5.6
	stat + syst	2.8	4.4	7.5
δ_{κ_λ}	stat only	3.4	4.8	7.4
	stat + syst	3.8	5.9	10.0

- Sensitivity driven by $b\bar{b}\gamma\gamma$
- **Systematics limited** (control of systematic needed)

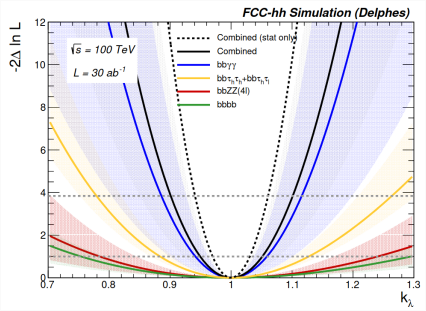

- Scenario I: optimistic, detector performance similar to Run-2
- Scenario II: realistic, intermediate
- Scenario III: conservative (pessimistic), extrapolated from HL-LHC performances

Systematics scenarios

parameterisation	scenario I	scenario II	scenario III
b-jet ID eff.	82-65%	80-63%	78-60%
b-jet c mistag	15-3%	15-3%	15-3%
b-jet l mistag	1-0.1%	1-0.1%	1-0.1%
τ-jet ID eff	80-70%	78-67%	75-65%
τ-jet mistag (jet)	2-1%	2-1%	2-1%
τ-jet mistag (ele)	0.1-0.04%	0.1-0.04%	0.1-0.04%
γ ID eff.	90	90	90
jet $\rightarrow \gamma$ eff.	0.1	0.2	0.4
$m_{\gamma\gamma}$ resolution [GeV]	1.2	1.8	2.9
m_{bb} resolution [GeV]	10	15	20

Prospect in e^+e^- collider

- directly accessible via ZHH and $\nu\bar{\nu}$HH
- $\delta^{\text{ILC}}(1\text{ TeV}) = 10\%$, $\delta^{\text{CLIC}}(3\text{ TeV}) = 9\%$

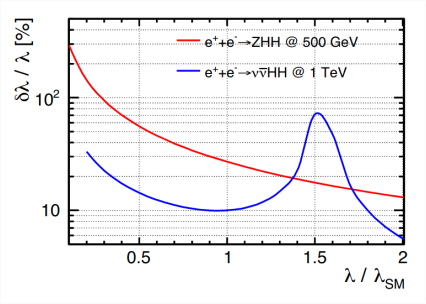

Knowledge from κ_λ

- **50% sensitivity** $\rightarrow$ reject $\kappa_\lambda = 0$ at 95%
- **20% sensitivity** $\rightarrow$ 5σ discovery of SM HH
- **5% sensitivity** $\rightarrow$ sensitive to quantum corrections to Higgs potential
- Precise measurement of κ_λ at FCC-hh requires precise knowledge of κ_t
- 1% κ_t leads to 5% κ_λ
- precise measurement of κ_t needs FCC-ee

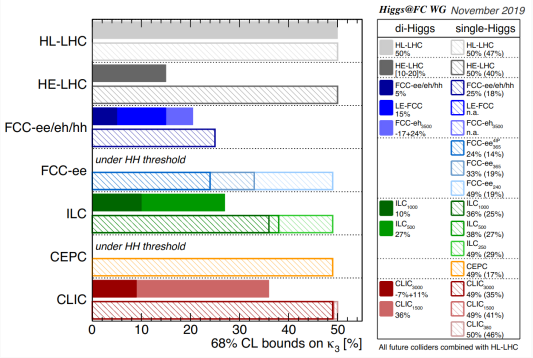

CNN architecture

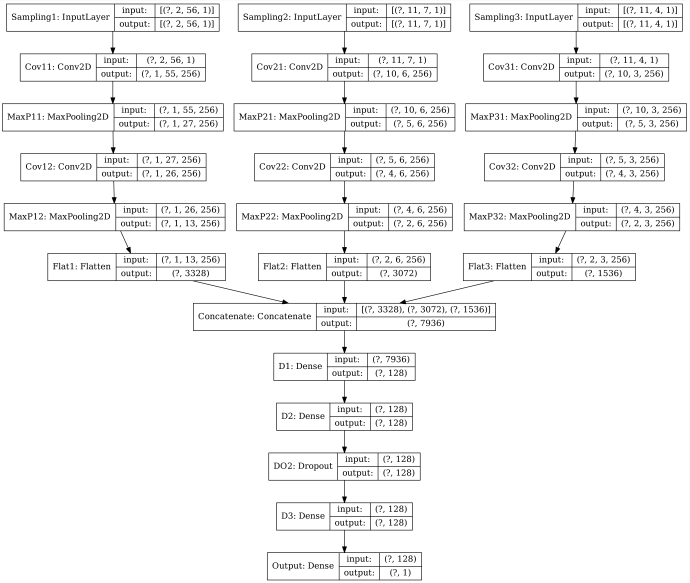

CNN images size

$\lvert\eta\rvert$ range	0 to 1.4	1.4 to 1.8	1.8 to 2.0	2.0 to 2.5
Sampling 1	112	112	84	56
Sampling 2	77	77	77	77
Sampling 3	44	44	44	44

Table 1: Number of cells in 7×11 EM calorimeter windows.

Sampling	Shape
Sampling 1	(56, 2)
Sampling 2	(7, 11)
Sampling 3	(4, 11)

Table 2: Image shape of 7×11 windows in each sampling in (η, ϕ).

Example of training images

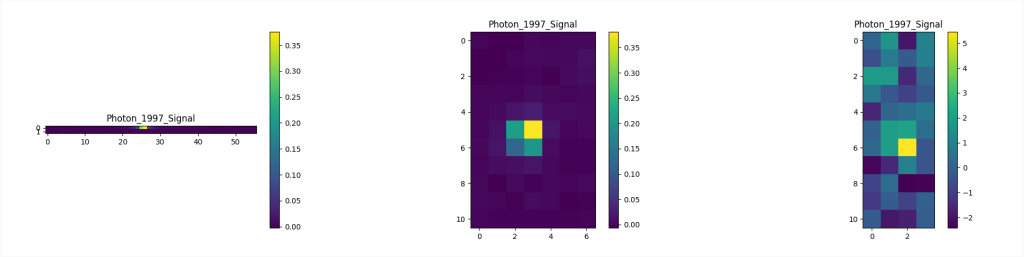

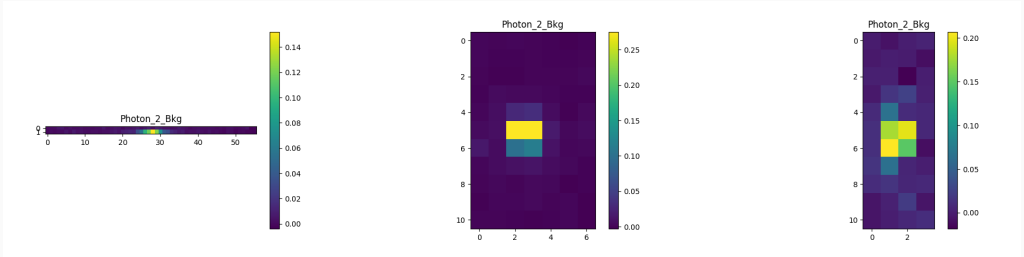

CNN vs DNN for photon identification

- SS-DNN trained on shower shapes variables
- CNN trained using images

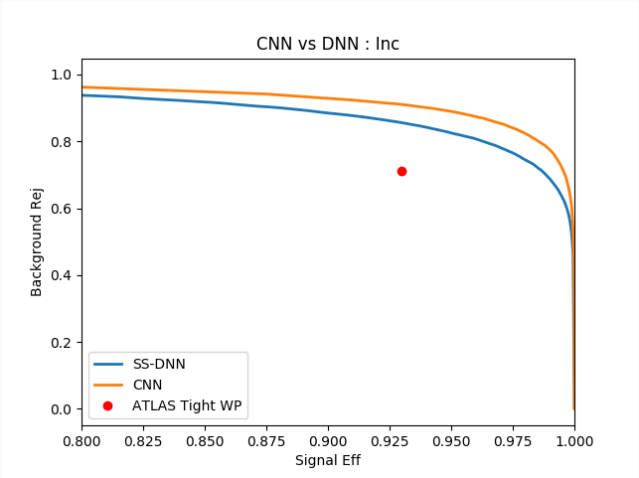

CNN performance compared to cut-based

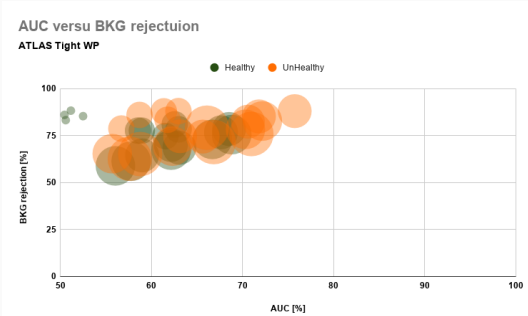

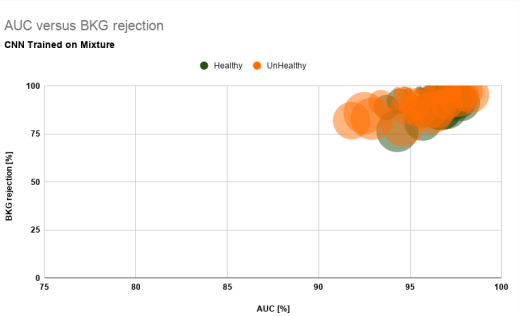

CNN signal improvement

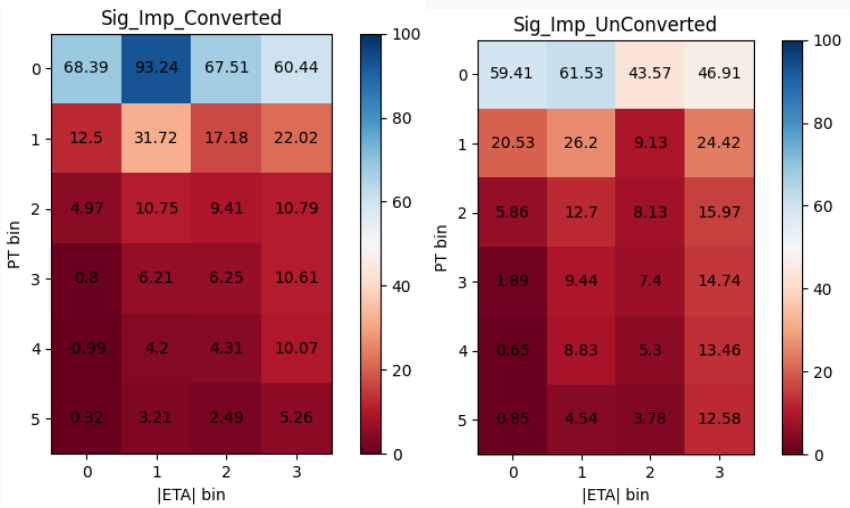

$p_T = [10, 20, 30, 40, 60, 80, \infty]$, $|\eta| = [0, 0.6, 1.37, 1.52, 1.8, 2.4]$

CNN background rejection

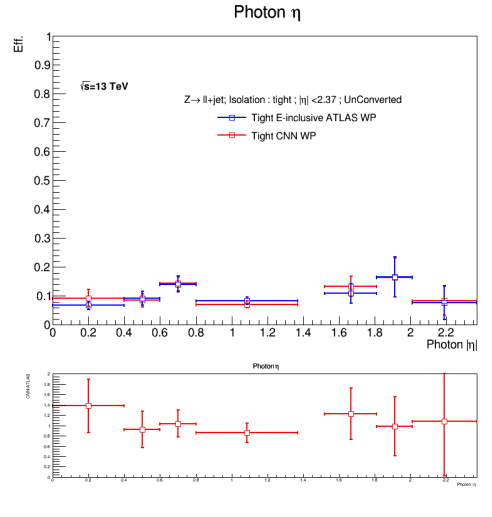

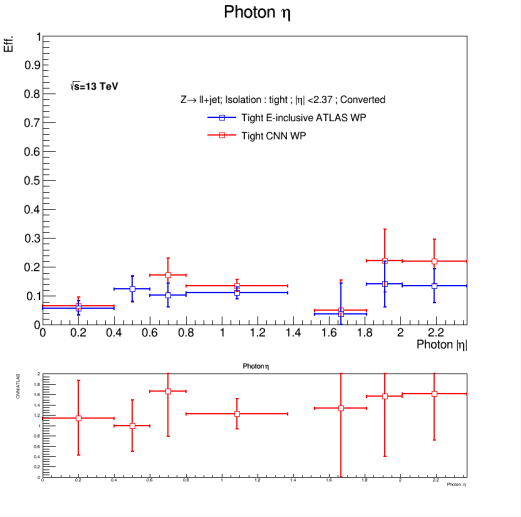

CNN efficiency, $|\eta| < 0.6$

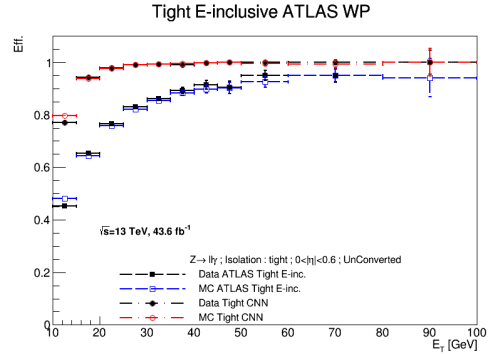

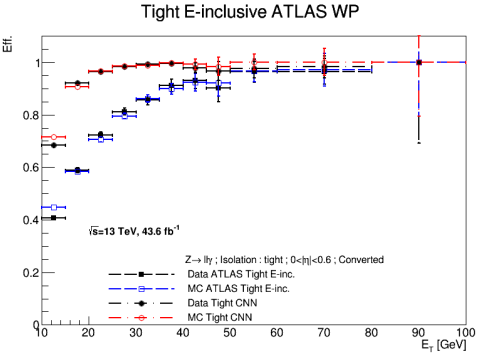

CNN efficiency, $0.6 < |\eta| < 1.37$

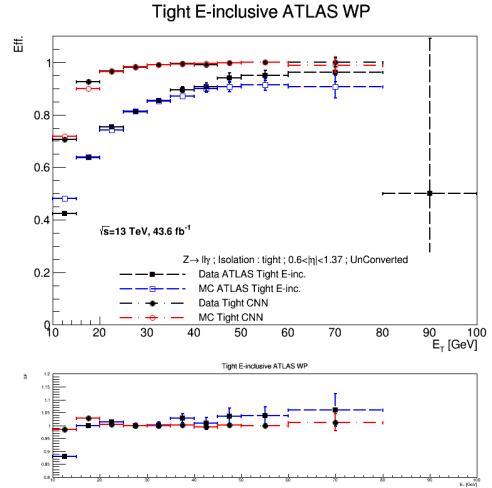

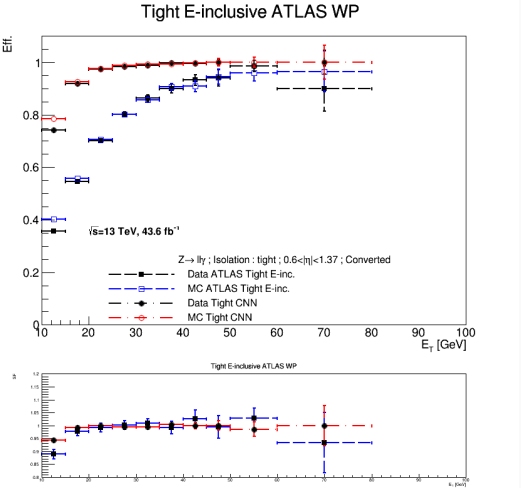

CNN efficiency, $1.81 < |\eta| < 2.01$

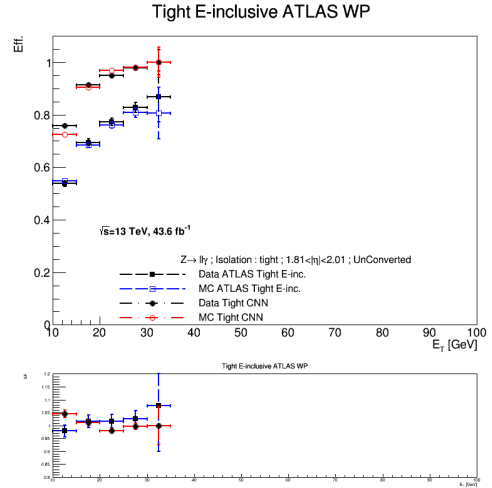

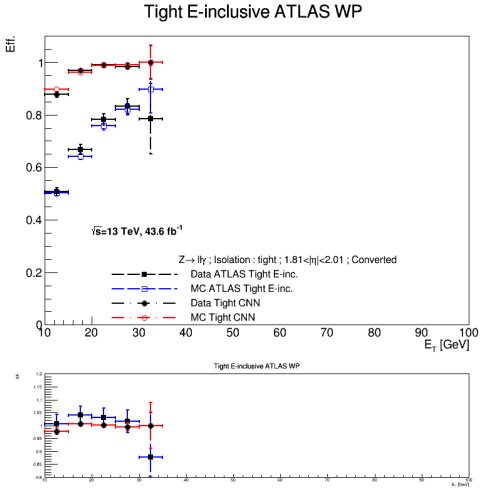

CNN efficiency, $2.01 < |\eta| < 2.37$

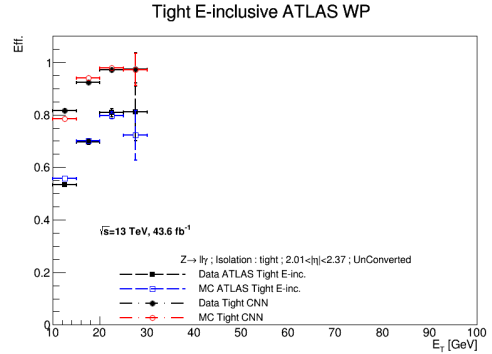

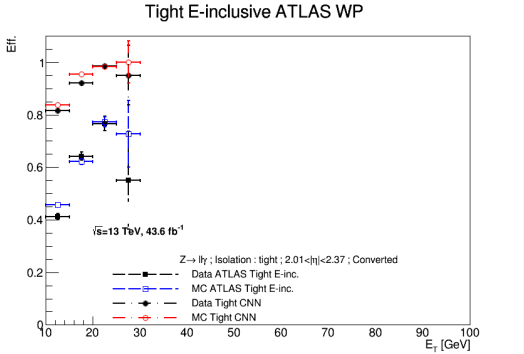

photon purity before CNN cut

	Unconverted			Converted		
	$ee\gamma$	$\mu\mu\gamma$	$ll\gamma$	$ee\gamma$	$\mu\mu\gamma$	$ll\gamma$
$10 < E_T < 15$	98.1±4.7	96.2±1.9	96.6±1.8	97.8±7.7	95.7±3.4	96.2±3.1
$15 < E_T < 20$	99.4±12.7	99.1±5.1	90.7±1.9	99.3±20.2	98.7±7.5	98.8±6.9
$20 < E_T < 25$	99.5±24.2	99.6±10.3	99.6±9.5	99.2±29.4	99.4±13.3	99.2±11.2
$25 < E_T < 30$	99.4±33.8	99.7±15.2	99.7±14.5	99.3±51.4	99.5±19.1	99.5±18.2
$30 < E_T < 100$	99.1±33	99.7±17.8	99.7±16.5	99.1±50.8	99.6±23.4	99.5±21.4

Table 3: Fitted photon purity in % of all probes, before tight CNN WP. The uncertainties are only statistical.

photon purity after CNN cut

	Unconverted			Converted		
	$ee\gamma$	$\mu\mu\gamma$	$ll\gamma$	$ee\gamma$	$\mu\mu\gamma$	$ll\gamma$
$10 < E_T < 15$	99.6±11.2	98.9±4.1	99.1±3.8	99.3±16.1	98.5±6.4	98.7±6.02
$15 < E_T < 20$	99.8±23.1	99.7±8.9	99.7±8.1	99.7±34.1	99.6±13.2	99.6±12.0
$20 < E_T < 25$	99.8±38.1	99.8±15.2	99.8±14.1	99.7±46.6	99.6±17.9	99.7±18.1
$25 < E_T < 30$	99.7±49.1	99.8±18.8	99.8±18.5	99.6±66.1	99.7±25.6	99.7±25.
$30 < E_T < 100$	99.5±45.6	99.8±21.2	99.8±20.7	98.9±49.4	99.7±28.5	99.7±25.8

Table 4: Fitted photon purity in % of all probes, after tight CNN WP. The uncertainties are only statistical.

scale factors for unconverted

	$0 < \|\eta\| < 0.6$	$0.6 < \|\eta\| < 1.37$	$1.81 < \|\eta\| < 2.01$	$2.01 < \|\eta\| < 2.37$
$10 < E_T < 15$	0.965 ± 0.0046	0.984 ± 0.0051	1.045 ± 0.0155	1.04 ± 0.011
$15 < E_T < 20$	1.01 ± 0.0032	1.03 ± 0.0036	1.01 ± 0.0114	0.982 ± 0.008
$20 < E_T < 25$	1.002 ± 0.0026	1.003 ± 0.003	0.980 ± 0.0099	0.992 ± 0.0093
$25 < E_T < 30$	0.999 ± 0.0025	0.998 ± 0.003	0.997 ± 0.0114	1.001 ± 0.091
$30 < E_T < 35$	0.999 ± 0.0032	0.999 ± 0.0032	1 ± 0.0746	
$35 < E_T < 40$	0.996 ± 0.0051	1.002 ± 0.0043		
$40 < E_T < 45$	0.999 ± 0.0067	0.995 ± 0.0077		
$45 < E_T < 50$	1 ± 0.0086	1.001 ± 0.0093		
$50 < E_T < 60$	1.004 ± 0.0114	1 ± 0.0097		
$60 < E_T < 80$	1.006 ± 0.0179	1.012 ± 0.0326		
$80 < E_T < 100$	1 ± 0.07			

Table 5: Scale factors for tight CNN WP efficiency measured with unconverted photons from $Z \to ll\gamma$ decays, in various bins of pseudorapidity and transverse energy. The uncertainty includes only statistical components.

scale factors for converted

	$0 < \|\eta\| < 0.6$	$0.6 < \|\eta\| < 1.37$	$1.81 < \|\eta\| < 2.01$	$2.01 < \|\eta\| < 2.37$
$10 < E_T < 15$	0.96 ± 0.012	0.944 ± 0.0085	0.978 ± 0.013	0.973 ± 0.013
$15 < E_T < 20$	1.02 ± 0.008	0.99 ± 0.006	1.008 ± 0.01	0.963 ± 0.011
$20 < E_T < 25$	0.999 ± 0.0067	0.99 ± 0.0044	1.001 ± 0.008	1.003 ± 0.012
$25 < E_T < 30$	0.999 ± 0.0063	0.995 ± 0.0044	0.994 ± 0.014	0.95 ± 0.137
$30 < E_T < 35$	1.007 ± 0.0079	0.995 ± 0.0054	1 ± 0.089	
$35 < E_T < 40$	0.997 ± 0.0114	1.004 ± 0.0066		
$40 < E_T < 45$	0.987 ± 0.0277	0.998 ± 0.012		
$45 < E_T < 50$	0.983 ± 0.0508	$1. \pm 0.018$		
$50 < E_T < 60$	0.976 ± 0.0455	0.99 ± 0.0279		
$60 < E_T < 80$	0.983 ± 0.0654	$1. \pm 0.078$		
$80 < E_T < 100$	1 ± 0.37			

Table 6: Scale factors for tight CNN WP efficiency measured with converted photons from $Z \to ll\gamma$ decays, in various bins of pseudorapidity and transverse energy. The uncertainty includes only statistical components.

Pile-up effect on CNN

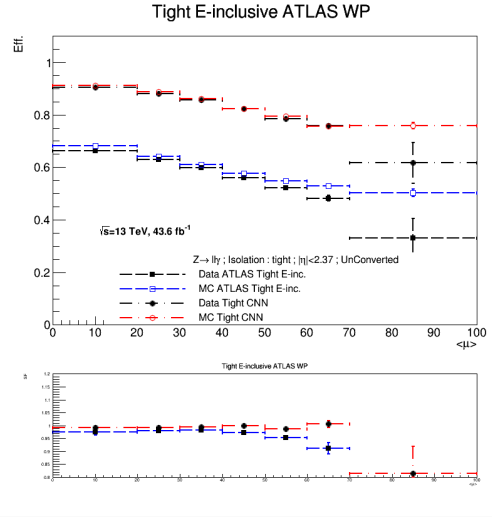

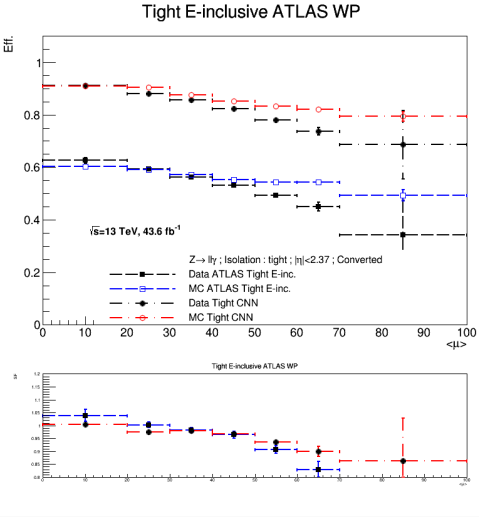

Primary verticies effect on CNN

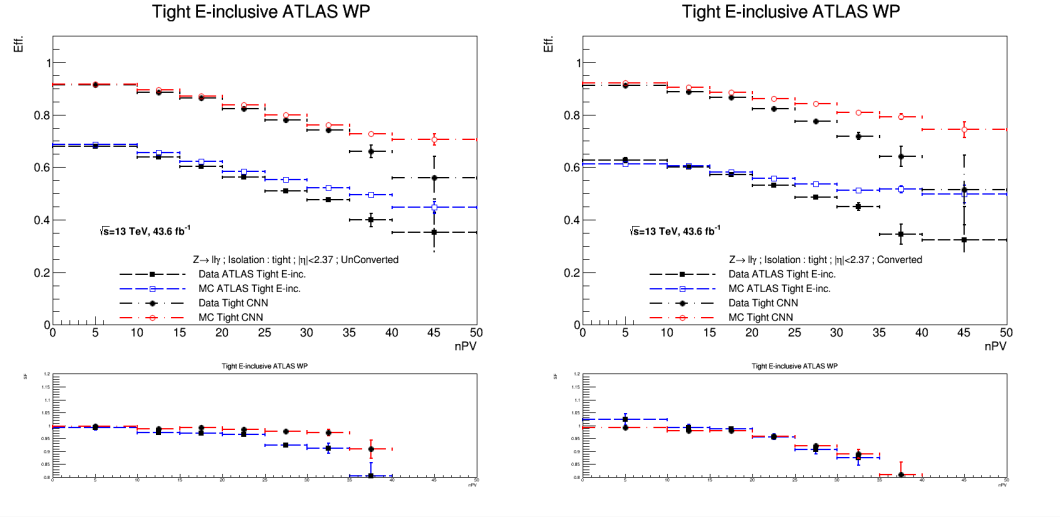

CNN output distribution, $|\eta| < 0.4$

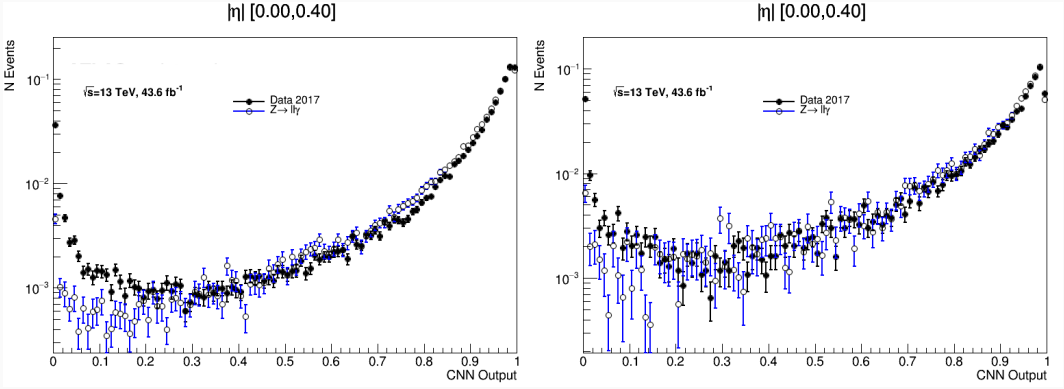

CNN output distribution, $0.4 < |\eta| < 0.6$

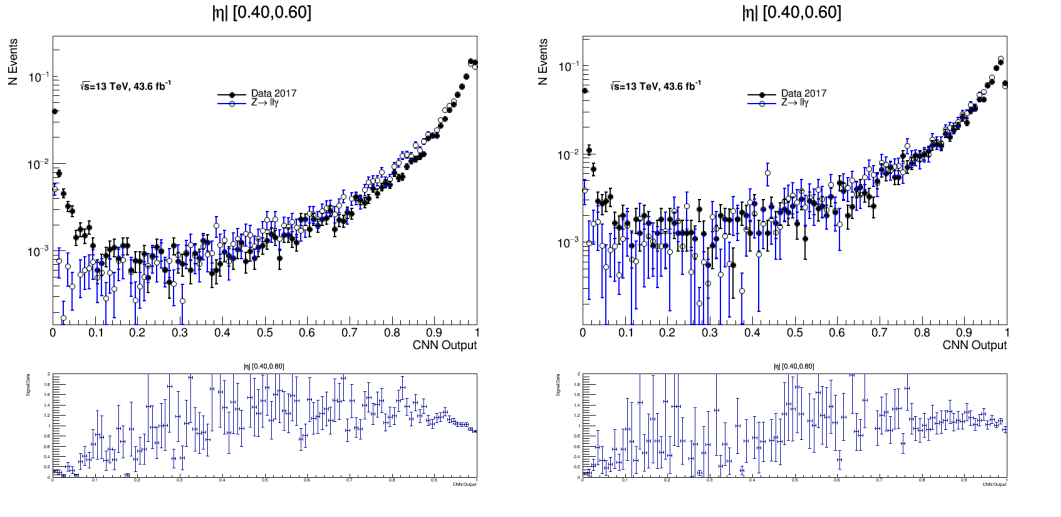

CNN output distribution, $0.6 < |\eta| < 0.8$

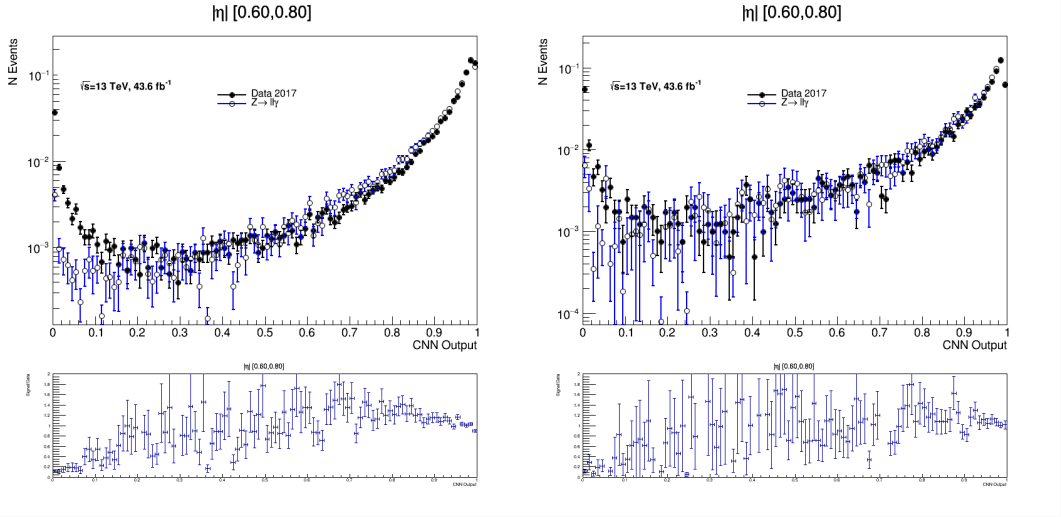

CNN output distribution, $0.6 < |\eta| < 1.37$

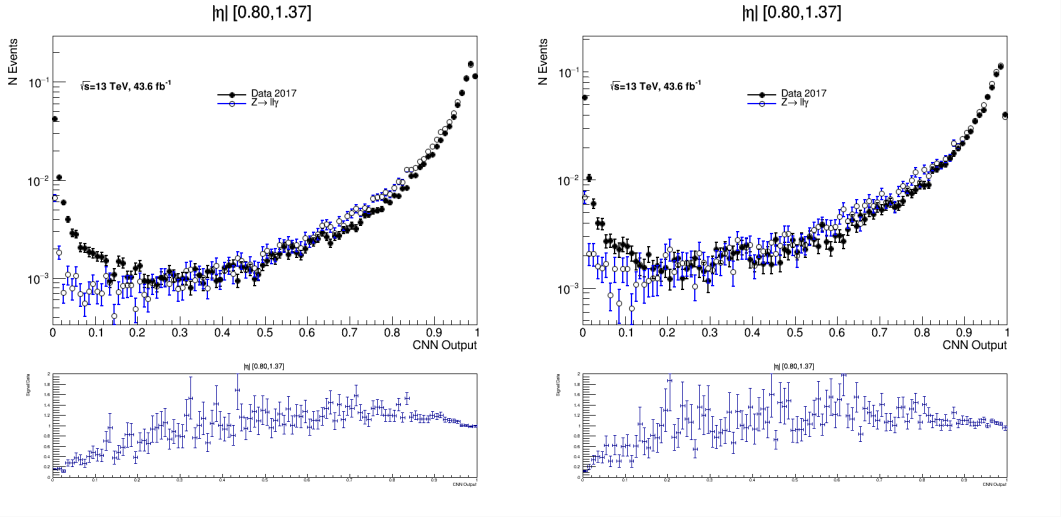

CNN output distribution, $1.52 < |\eta| < 1.81$

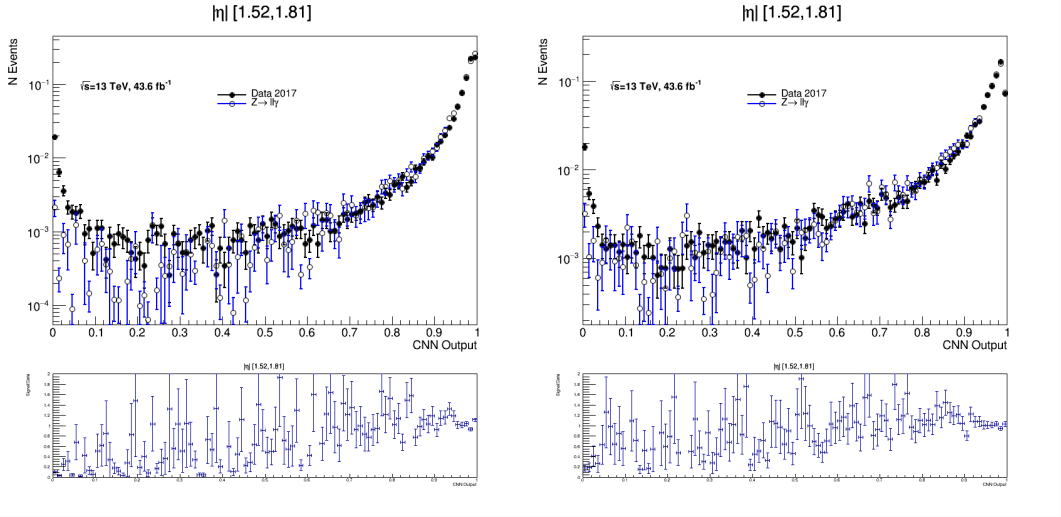

CNN output distribution, $1.81 < |\eta| < 2.01$

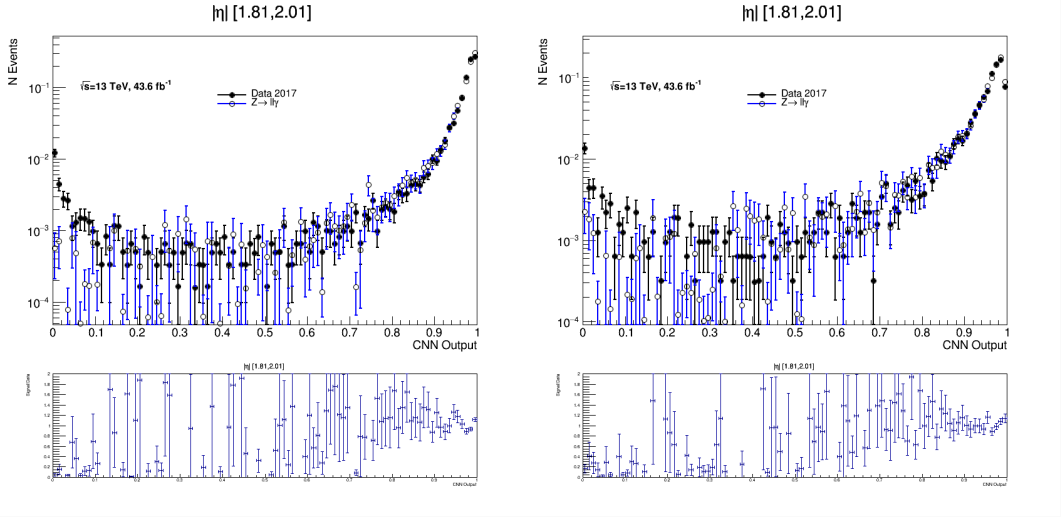

CNN output distribution, $2.01 < |\eta| < 2.37$

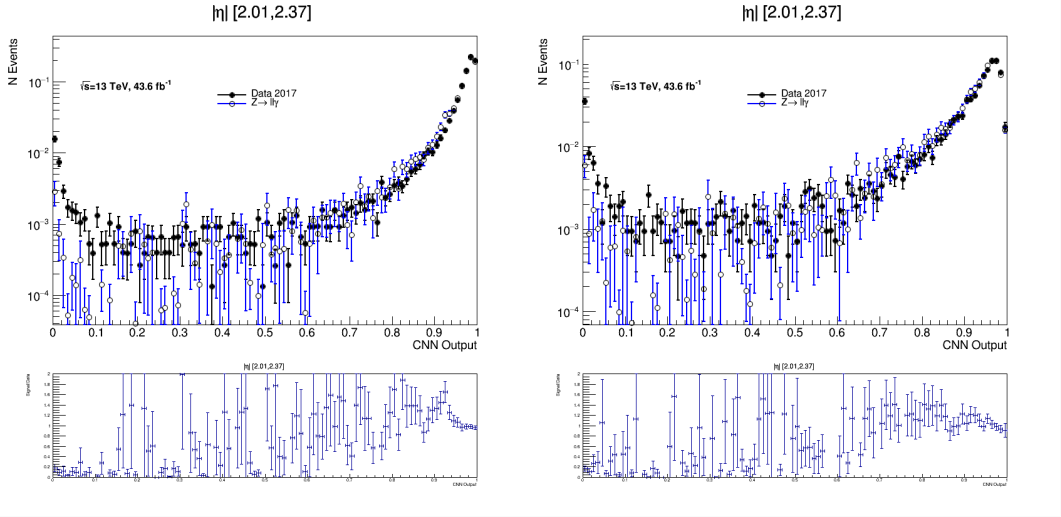

Low efficiency at High $|\eta|$

- CNN performances degrades at low p_T and high η:
  - low energy photons deposit more energy in the first layer.
  - first layer granularity at high $|\eta|$.
- **Take into account η during the training**

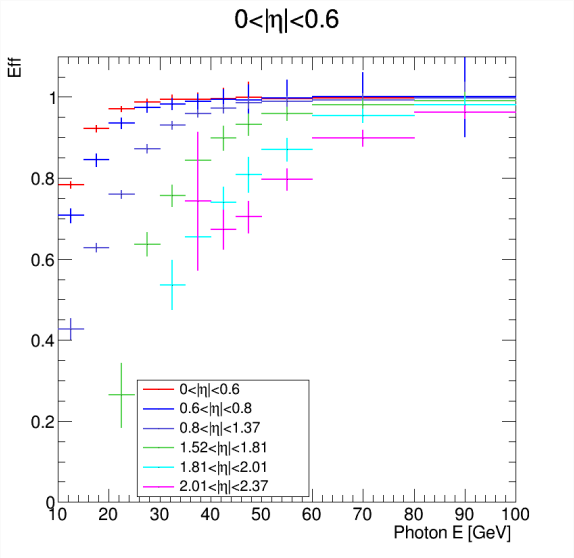

Multi-Task Cascade Convolutional Network (MTCNN)

- Alternative solution for considering photons direction.
- Used in face detection.
- Can be used with topological clusters.

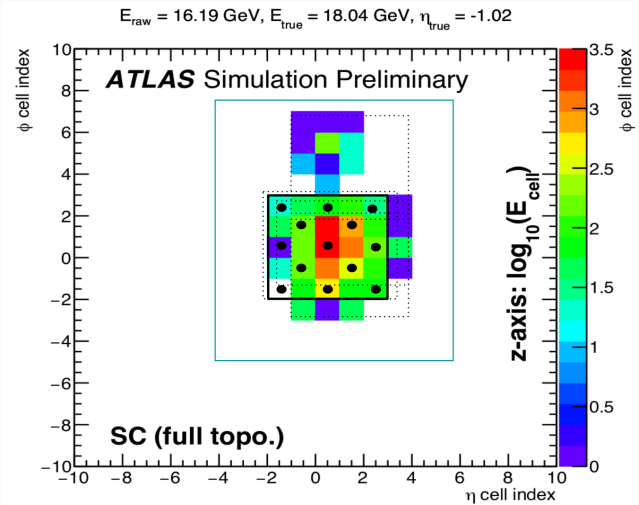

Pile-Up Auto-Encoder Denoising

- Efficiency degradation for increasing the Pile-Up (crucial at HL-LHC).
- Medicine (image denoising) $\rightarrow$ ATLAS (pile-up denoising).
- Learn the laten representation of the image using an Auto-Encoder.

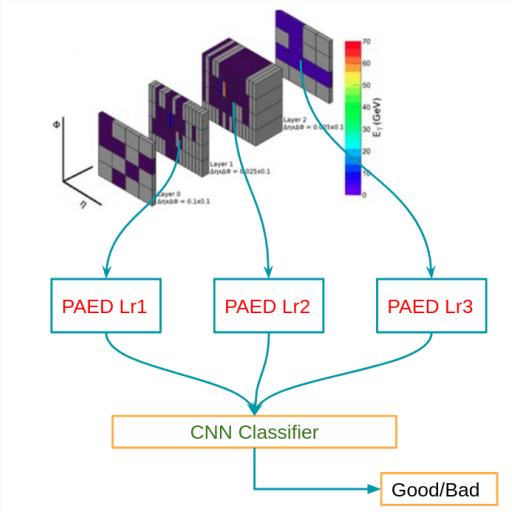

Cell energy vs Cell energy fraction

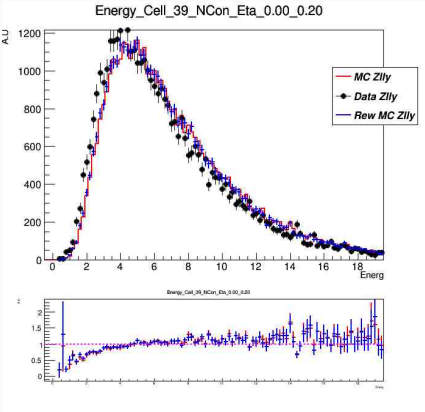

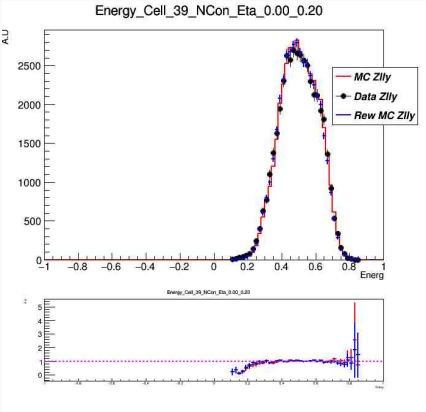

Kinematic Fit

- Consist of calibration of the HH system balance in the transverse plan.
- Profit from $m_{\gamma\gamma}$ resolution to improve m_{bb} resolution.
- Constrain the $P_{x,y}^{HH+jets}$, using a likelihood, since additional jets are an important part of HH system.

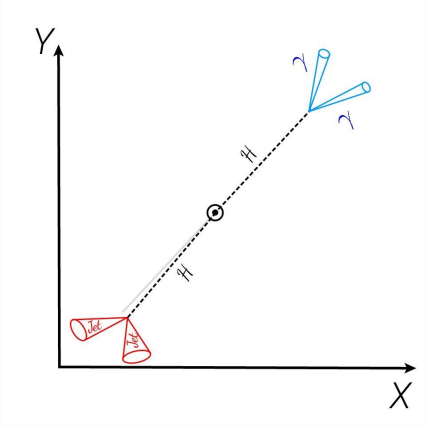

$$-2\log(\mathcal{L}) = \sum_i \left(\frac{\Omega_i^* - \Omega_i}{\sigma_{\Omega_i}}\right)^2 - 2\log\left(L\left(p_T\right)\right) + \left(\frac{\sum p_x^* - 0}{\sigma_{\sigma_{bb\gamma\gamma}}}\right)^2 + \left(\frac{\sum p_y^* - 0}{\sigma_{\sigma_{b\bar{b}\gamma\gamma}}}\right)^2$$

$\sigma_{b\bar{b}\gamma\gamma}$ determination

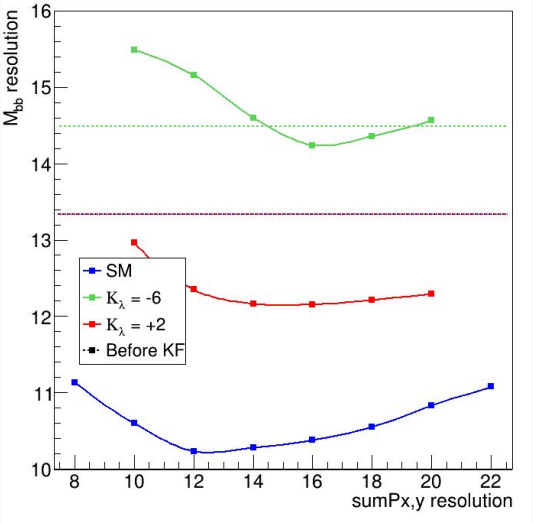

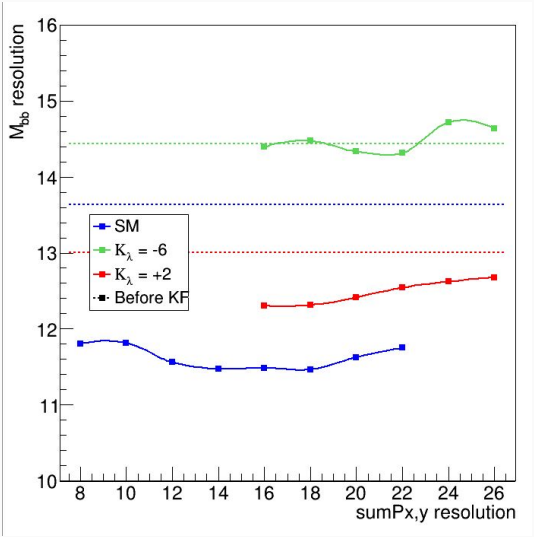

HH system balance

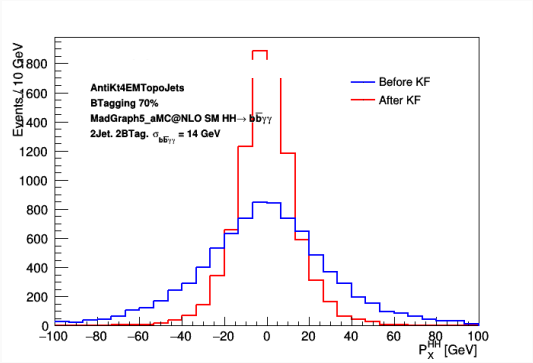

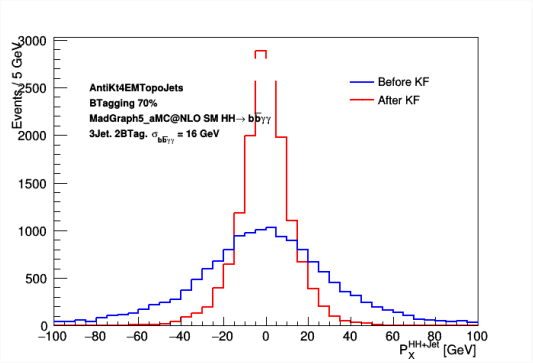

m_{bb} improvement